Biased M1-muscarinic receptor mutant mice inform design of next generation drugs

Sophie J. Bradley[1]*, Colin Molloy[1], Paulina Valuskova[1,] Louis Dwomoh[1], Miriam Scarpa[1], Mario Rossi[1], Lisa Finlayson[1], Kjell A. Svensson[3], Eyassu Chernet[3], Vanessa N. Barth[3], Karolina Gherbi[4,6], David A. Sykes[4,5], Caroline A. Wilson[7], Raj Mistry[8], Patrick M. Sexton[9], Arthur Christopoulos[9], Adrian J. Mogg[3], Elizabeth M. Rosethorne[4,5], Shuzo Sakata[7], R. A. John Challiss[8], Lisa M. Broad[2] and Andrew B. Tobin[1]*

[1] The Centre for Translational Pharmacology, Institute of Molecular, Cell and Systems Biology, College of Medical, Veterinary and Life Sciences, University of Glasgow, Glasgow, G12 8QQ, UK.

[2] Eli Lilly & Co, Neuroscience Discovery, Erl Wood Manor, Windlesham, Surrey, GU20 6PH, UK.

[3] Eli Lilly & Co, Neuroscience Discovery, Lilly Corporate Center, Indianapolis, Indiana, USA.

[4] School of Life Sciences, Queen's Medical Centre, University of Nottingham, Nottingham, NG7 2UH, UK.

[5] Centre of Membrane and Protein and Receptors (COMPARE), University of Birmingham and University of Nottingham, Midlands, UK.

[6] Excellerate Bioscience Ltd, BioCity, Pennyfoot Street, Nottingham, NG1 1GF, UK.

[7] Strathclyde Institute of Pharmacy and Biomedical Sciences, University of Strathclyde, 161 Cathedral Street, Glasgow, G4 0RE, UK.

[8] Department of Molecular and Cell Biology, Henry Wellcome Building, University of Leicester, Lancaster Road, Leicester, LE1 7RH, UK.

[9] Drug Discovery Biology, Monash Institute of Pharmaceutical Sciences and Department of Pharmacology, Monash University, Parkville, Victoria, 3052, Australia.

* Corresponding authors: Andrew B. Tobin and Sophie J Bradley

Abstract

Cholinesterase inhibitors, the current frontline symptomatic treatment for Alzheimer's disease (AD), are associated with low efficacy and adverse effects. M1 muscarinic acetylcholine receptors (M1 mAChRs) represent a potential alternative therapeutic target; however, drug discovery programmes focused on this G protein-coupled receptor (GPCR) have failed largely due to cholinergic adverse responses. Employing novel chemogenetic and phosphorylation-deficient, G protein-biased, mouse models, paired with a tool-box of probe molecules, we establish previously unappreciated pharmacologically targetable M1 mAChR neurological processes, including anxiety-like behaviours and hyper-locomotion. By mapping the upstream signalling pathways regulating these responses, we determine the importance of receptor phosphorylation-dependent signalling in driving clinically relevant outcomes and in controlling adverse effects including *"epileptic-like"* seizures. We conclude that M1 mAChR ligands that promote receptor-phosphorylation dependent signalling would protect against cholinergic-adverse effects in addition to driving beneficial responses such as learning and memory and anxiolytic behaviour relevant for the treatment of AD.

Introduction

Alzheimer's disease (AD) is the most common form of dementia affecting ~850,000 people in the UK alone, and 50 million worldwide. Like many forms of dementia, AD is associated with a spectrum of symptoms that includes memory loss but also behavioural disturbances, such as anxiety and agitation. A single treatment strategy that might address the multiple components of AD has yet to emerge. Rather the underlying basis of symptomatic treatment of AD is centred on addressing cognitive deficits by the restoration of cholinergic transmission via the inhibition of acetylcholinesterase, the enzyme responsible for the breakdown of acetylcholine [1]. However, the efficacy of this treatment is limited by serious dose-related cholinergic adverse responses due primarily to the whole-body up-regulation of cholinergic systems, both central and peripheral [2,3].

A widely considered alternative strategy has been to target the M1 mAChR, one of five members (M1-M5) of a family of G protein-coupled receptors (GPCRs) that respond to acetylcholine and that shows pro-cognitive effects in preclinical animal studies [4-8]. However, despite some positive indications of efficacy in clinical trials, the M1/M4 preferring orthosteric agonist xanomeline[9] and the bitopic agonist GSK1034702 [10-12], failed due to adverse cholinergic effects. An alternative strategy, designed to reduce adverse responses by increasing selectivity for the M1 mAChR, is to target non-conserved allosteric sites which would positively modulate receptor activity, so called positive allosteric modulators (PAMs) [13]. Despite the discovery of a variety of structurally distinct M1 mAChR-selective PAMs [7] some of these molecules have similarly run into issues regarding adverse responses that include temporal lobe seizures [7,14,15]. These studies highlight the serious lack of appreciation of the subtle pharmacological and structural properties of both M1-selective PAMs and

orthosteric/bitopic ligands that underlie clinically efficacious responses versus adverse outcomes [10,15,16].

Furthermore, the potential of utilising the concept of biased signalling [17] to avert muscarinic adverse responses that have thwarted drug discovery has similarly lacked thorough investigation [18]. In order to realise the full potential of M1 mAChR biased ligands, it will be necessary to dissect the *in vivo* signalling pathways that mediate clinically relevant M1 mAChR neurological processes, and distinguish these from pathways leading to adverse responses [17]. We address this challenge here by generating a G protein-biased M1 mAChR by removing receptor phosphorylation sites and thereby uncoupling the receptor from phosphorylation/arrestin-dependent signalling. By knock-in of this G protein-biased receptor (M1-PD) into the gene locus of the wild type M1 mAChR, we were able to assign neurological and peripheral responses to either G protein-dependent or receptor phosphorylation/arrestin-dependent signalling.

We combined this approach with a unique application of **D**esigner **R**eceptor **E**xclusively **A**ctivated by **D**esigner **D**rug (DREADD) technology, where the introduction of mutations in transmembrane domains 3 and 5 of the M1 mAChR generated a receptor mutant (M1-DREADD) that was unresponsive to the natural ligand acetylcholine, but rather was activated by the otherwise inert chemical ligand clozapine-N oxide (CNO)[19]. Whereas many other studies have used muscarinic DREADDs to investigate the role of G protein signalling in neuronal processes [20], here by knock-in of the M1-DREADD coding sequence into the M1 mAChR gene locus we express the M1-DREADD in place of the wild type M1 mAChR in a study designed to define the role and "*druggablilty*" of the M1 mAChR. We predicted that the phenotype of this mutant mouse would mimic that of the M1-receptor knockout

(M1-KO) mice since the M1-DREADD receptor does not respond to acetylcholine. However, unlike M1-KO mice, deficits resulting from a loss of M1 mAChR activity would be corrected in the M1-DREADD mice by treatment with CNO. In this way we reasoned we could define physiological responses that might be targetable by pharmacological activation of the M1 mAChR. Using this approach together with the M1-PD mice and a mouse line expressing a phosphorylation-deficient version of the M1-DREADD (M1-DREADD PD) we describe here that pharmacological targeting of the M1 mAChR not only impacts on learning and memory but can also correct disturbances in anxiety-related behaviours and hyperactivity, suggesting that M1 mAChR ligands hold the promise of treatment of a broad spectrum of symptoms associated with AD. By mapping the bimodal signalling pathways underlying neurological and adverse responses of the M1 mAChR we further conclude that ligands biased towards M1 mAChR phosphorylation/arrestin-dependent signalling will have efficacy in clinically-relevant responses, while minimising adverse effects including *"epileptic-like"* seizures.

Results

Generation of the M1-DREADD mice

Consistent with previous studies[19], the human wild type M1 mAChR expressed in Chinese hamster ovary (CHO) cells was potently activated by acetylcholine while showing a weak response to CNO, in an inositol phosphate accumulation assay **(Supplementary Table 1)**. CHO cells expressing the M1-DREADD receptor showed a significant (5000-fold) reduction in the potency of acetylcholine while responding to CNO with nM potency **(Supplementary Table 1)**. Targeting the M1 mAChR gene locus with a construct that, following homologous recombination, replaced the coding sequence of the M1 mAChR with the coding sequence of the M1-DREADD **(Figure 1A and Supplementary Figure 1 A-C)** resulted in mice that transcribed the M1-DREADD mRNA in the hippocampus and cortex at levels that were not significantly different from that of the M1 mAChR in wild type animals (which refers to animals that express a wild type M1 mAChR tagged at the C-terminus with an HA-epitope tag) **(Figure 1B)**. Furthermore, the M1-DREADD protein was expressed at comparable levels to that of the wild type receptor in the cortex of control mice, but slightly higher levels in the hippocampus **(Figure 1C-D, Supplementary Figure 2)**. The M1-DREADD mice showed normal levels of breeding and indicators of good health.

To establish the sensitivity of the M1-DREADD expressed in the engineered mice to muscarinic ligands, coupling of the M1-DREADD to heterotrimeric G proteins was assessed in membranes prepared from the cortex. In these experiments, CNO showed no significant activity in cortical membranes prepared from wild type animals, while the muscarinic agonist carbachol produced a robust increase in [^{35}S]GTPγS binding **(Figure 1E, Supplementary Table 2).** In contrast, CNO

produced a potent increase in $G_{q/11}$-coupling in cortical membranes prepared from M1-DREADD mice while carbachol failed to stimulate a response **(Figure 1F, Supplementary Table 2).**

Hence, the M1-DREADD in our engineered mice was expressed near equivalently to that of the M1 mAChR in wild type mice and was not activated by the natural ligand acetylcholine, but was instead activated by CNO.

CNO reduces hyper-anxiety levels in M1-DREADD mice

M1-KO animals showed an increased anxiety-like phenotype in an elevated plus maze (EPM) test as demonstrated by significantly fewer entries into the open arms of the maze compared to controls **(Figure 2A-G)**. M1-DREADD mice similarly showed fewer entries into the open arms of the maze (relative to total entries) compared to controls, indicating that the M1-DREADD animals mimicked the phenotype of the M1-KO mice **(Figure 2A-G)**. The hyper-anxiety phenotype shown by the M1-DREADD mice was restored to normal levels by the administration of CNO (0.3 mg/kg) 30 min prior to the behavioural test **(Figure 2 A-G)**. Previous pharmacokinetic studies from our laboratory determined that 0.3 mg/kg CNO administration (i.p.) gave a plasma exposure of approximately 50 nM [21], a concentration sufficient to fully activate virally expressed muscarinic DREADDs *in vivo*. Importantly, CNO (0.3 mg/kg; i.p.) had no effects on the wild type mice nor the M1-KO mice in the EPM **(Figure 2 A-G).** These data indicate that loss of M1-AChR function results in an anxiety-like phenotype that is restored by direct activation of M1 mAChRs through selective ligands.

Hyperactivity of M1 DREADD mice is restored by CNO

Consistent with previous studies [22] we confirm that M1-KO mice are hyperactive in an open field test. **(Figure 2H-K** *(also see;* ***Figure 4E and G-K*** *below)***).** Since M1-DREADD is not responsive to the natural ligand, acetylcholine, mice expressing the M1-DREADD similarly displayed a hyper-locomotion phenotype **(Figure 2H-K)**. The hyper-locomotion associated with both M1-KO and M1-DREADD animals was also evident when the mice were tested in a Y maze paradigm **(Figure 2L and Supplementary Figure 3).** Importantly, administration of CNO (0.3mg/kg) had no significant effects on the locomotion of wild type or M1-KO mice, but reduced the hyper-locomotion observed in M1-DREADD animals to levels similar to that seen in vehicle-treated control animals **(Figure 2G and L and Supplementary Figure 3)**. These data indicate that not only are M1 mAChRs involved in regulating locomotion, but that modulation of locomotion is *"druggable"* via selective agonism of this receptor subtype.

Generation of a phosphorylation-deficient M1 mAChR mouse

Like many other GPCRs, muscarinic receptors operate through two signalling arms namely, via heterotrimeric G proteins and receptor phosphorylation regulated pathways[23]. The latter includes receptor coupling to arrestin-adaptor proteins and activation of arrestin-dependent processes such as receptor internalisation[24]. A mutant M1 mAChR that lacked all of the mass spectrometry identified phosphorylation sites[25] and other potential sites in the third intracellular loop and C-terminal tail (20 serine–alanine substitutions in total) **(Figure 3A)**, was generated and expressed in HEK-293 cells. This mutant receptor showed robust coupling to $G_{q/11}$/calcium mobilisation **(Figure 3B, Supplementary Table 3)** while showing

reduced agonist-mediated receptor recruitment of arrestin **(Figure 3C, Supplementary Table 3)** and a deficit in receptor internalisation **(Figure 3D, Supplementary Figure 4)**. These results are consistent with the notion that the phosphorylation-deficient receptor is *"G protein-biased"*.

A receptor knock-in mouse that expressed the phosphorylation-deficient form of the mouse M1 mAChR was generated, termed M1-PD **(Supplementary Figure 5).** By comparing this mouse line with wild type controls (that express a C-terminally tagged wild type M1 mAChR) and M1-KO animals, it was our aim to differentiate between physiological responses that lie downstream of receptor phosphorylation-dependent signalling and those mediated by G protein activation**.** Radioligand binding assays determined that muscarinic receptor expression in M1-PD mice in the cortex was equivalent to that in wild type mice **(Figure 3E).** Transcription of the mutant receptor in the cortex and hippocampus of M1-PD mice was not significantly different from that of the M1 mAChR in control animals **(Figure 3F)** and quantification of Western blotting results revealed no significant difference in the expression levels of the mutant M1 mAChR in the hippocampus and cortex of M1-PD mice **(Figure 3G-H and Supplementary Figure 6).** Finally, the coupling to heterotrimeric G proteins (as determined in [^{35}S]GTPγS assays and inositol 1,4,5-trisphosphate mass assays) of the M1 mAChR and phosphorylation-deficient variant was equivalent in cortical tissue extracts **(Figure 3I-J, Supplementary Table 3).**

Neuro-physiology regulated by M1 mAChR phosphorylation

We first tested the anxiolytic response in the M1-PD mice and found that, similar to the M1-KO mice, the M1-PD mice showed fewer entries into the open arms of an EPM **(Figure 4A-E)**. This indicates that anxiolytic responses revealed in the studies

above are mediated by receptor phosphorylation-dependent signalling. Similarly, in a Y-maze spontaneous alternation paradigm testing spatial working memory, the M1-PD mice showed significant deficit indicating that like the M1 mAChR-mediated anxiolytic response, this behaviour is also under the positive regulation of receptor phosphorylation **(Figure 4F)**.

Locomotion was initially assessed in the open field test where M1-PD mice did not mimic the hyperactivity phenotype of M1-KO mice **(Figure 4G-J)**. Rather in this test **(Figure 4J)** and in the EPM **(Figure 4E)** the total distance travelled by the M1-PD mice was less than wild type indicating that these mice were hypo-active. Interestingly, although locomotion monitored over a 24 hour period using telemetry showed the M1-KO mice to be hyper-active, consistent with the above data, under this paradigm the M1-PD showed activity equivalent to wild type mice **(Figure 4K)**. The conclusion from these locomotion studies was that, in contrast to the anxiolytic and spatial working memory responses, regulation of locomotor behaviour is not dependent on receptor phosphorylation, but appears to be regulated in a G protein-dependent manner. The hypo-locomotion response observed in some of the tests (EPM and Y maze) might indicate that although mediated by G protein pathways, M1 mAChR locomotion might be desensitised by receptor phosphorylation resulting in hypo-locomotion when phosphorylation sites are removed **(see; Figure 4E and J).**

We next compared these central responses with M1-mAChR mediated salivary secretion. M1-KO mice showed reduced salivary secretion in response to the muscarinic receptor agonist pilocarpine, as previously described[26], but this was not mimicked by the M1-PD mice **(Figure 4L)** indicating that this response also is downstream of G protein-dependent signalling **(summarised in Figure 4M).**

M1 mAChR phosphorylation reduces adverse responses

To further probe the role of receptor phosphorylation-dependent signalling in M1 mAChR-mediated responses, an M1-DREADD receptor was generated where the phosphorylation sites had been removed **(Figure 5A)**. In *in vitro* inositol phosphate assays, this phosphorylation-deficient DREADD receptor was activated by CNO with similar potency and efficacy to the fully phosphorylatable version of M1-DREADD **(Supplementary Figure 7A, Supplementaty Table 1)**. Consistent with a role for receptor phosphorylation in driving phosphorylation/arrestin-dependent processes, the phosphorylation deficient M1-DREADD was defective in agonist (CNO) mediated receptor internalisation **(Supplementary Figure 7B-C).**

A knock-in mouse expressing the phosphorylation-deficient M1-DREADD in place of the M1 mAChR was generated and termed M1-DREADD PD **(Supplementary Figure 8A-B)**. The M1-DREADD PD mutant was transcribed at levels equivalent to that of the M1-DREADD receptor in M1-DREADD mice and the M1 mAChR in wild type mice **(Figure 5B)**.

Possibly due to the fact that the M1-DREADD receptor is not activated by endogenous acetylcholine, the levels of expression of this receptor in hippocampus (but not the cortex) of engineered mice were slightly higher than that of the wild type receptor **(Supplementary Figure 2).** The expression of M1-DREADD PD was also significantly higher than wild type receptor **(Figure 5C-D and Supplementary Figure 2).** Importantly, there were no statistically significant differences between the expression levels of M1-DREADD and M1-DREADD PD receptors in the hippocampus or cortex **(Supplementary Figure 2).** This is relevant since the M1-DREADD acts as the control for the M1-DREADD PD (we do not use wild type mice as controls when looking at the phenotype of the M1-DREADD PD).

G protein coupling assays in cortical membranes derived from M1-DREADD and M1-DREADD PD showed that CNO stimulated robust increases in $G_{q/11}$ coupling in both variants whereas carbachol gave no significant increases **(Figure 5E-F, Supplementary Table 2).** When normalised to expression levels we estimated that M1-DREADD PD signalling to G_q was ~1.5 fold higher than M1-DREADD.

CNO induces adverse responses in M1-DREADD PD mice

The aim here was to investigate if physiological responses mediated by CNO administration to animals expressing the M1-DREADD receptor were similarly responsive in M1-DREADD PD mice. In this way we might further predict the impact of biased M1 mAChR selective ligands. However, administration of CNO to M1-DREADD PD mice resulted in profound adverse responses **(Supplementary Table 4**) including both central and peripheral responses such as gastro-intestinal disturbances and salivary hyper-secretion. These adverse responses have previously been associated with the failure of muscarinic drug discovery programmes[9,12,14,27-30]. Most striking however was the severe seizures characteristic of cholinergic temporal lobe “epileptic-like” seizures [31-33]. We further characterised these seizures using surface EEG recordings to monitor cortical activity **(Figure 5G-H).** CNO induced a reduction in EEG power following CNO administration, followed by sporadic seizure activity, which subsequently developed into full epileptic-like episodes around 25-35 min after CNO administration. Importantly, the same dose of CNO (0.3 mg/kg) administered to M1-DREADD mice had no adverse effects **(Supplementary Table 4)**.

G protein biased systems show enhanced adverse responses

These data led to the prediction that a muscarinic-receptor ligand biased toward G protein-dependent signalling versus receptor phosphorylation-dependent signalling will show more adverse responses than a non-biased ligand. To test this prediction we profiled the G protein/receptor phosphorylation bias of two well-characterised muscarinic ligands, pilocarpine [31] and GSK1034702 [10-12]. Both these ligands stimulated $G_{q/11}$-dependent signalling to inositol phosphate accumulation and phosphorylation and activation of extracellular signal-regulated kinase 1/2 (pERK1/2) **(Figure 6A-B).** Similarly both pilocarpine and GSK1034702 stimulated phosphorylation of serine 228 in the third intracellular loop of the M1 mAChR, a site previously showed to be highly sensitive to agonist-mediated phosphorylation [25] **(Supplementary Table 5; Figure 6C).** Fitting the concentration response curves to the operational model of agonism we derived a transduction co-efficient (τ tau) for each of the responses. By comparing these with the transduction co-efficient of the natural ligand acetylcholine we calculated bias of the two ligands between G protein coupling and receptor phosphorylation which was expressed as a bias-factor **(Supplementary Table 6, Figure 6D).** This analysis determined that pilocarpine showed bias toward G protein signalling, whereas GSK1034702 showed no bias between G protein coupling and receptor phosphorylation pathways **(Supplementary Table 6, Figure 6D).**

That these ligands show similar properties *in vivo* was investigated by administration of either pilocarpine (30 mg/kg) or GSK1034702 (10 mg/kg) at doses that resulted in equivalent levels of receptor occupancy (60%) in rats, as determined using an M1 mAChR PET tracer, LSN3172176 [34] **(Supplementary Figure 9)**. At this dose pilocarpine resulted in a robust inositol phosphate response that was ~2 fold greater

than that observed for GSK1034702 **(Figure 6E-F),** supporting the conclusion that pilocarpine is more efficacious in stimulating G protein-dependent signalling compared to GSK1034702 in brain tissue.

We then examined adverse events in response to these two ligands in wild type and M1-PD mice using doses that gave equivalent receptor occupancy. Consistent with the notion that ligands biased towards G protein signalling would show more pronounced adverse responses, we observed that pilocarpine induced significant central (tremors, grasping and convulsions) and peripheral adverse responses (piloerection, lacrimation and diarrhoea) in both WT and M1-PD mice **(Supplementary Table 7)**. Interestingly, salivation was the only response that was lower in the M1-PD compared to WT in response to pilocarpine **(Supplementary Table 7).** Whereas this might point to salivation being downstream of receptor phosphorylation dependent signalling, the data in Fig 5L would point to this response being solely G protein mediated. In contrast to pilocarpine, GSK1034702, which showed no stimulus bias, also showed no adverse responses in WT mice. It is only in the M1-PD mice (i.e. in a mouse background where the receptor is G protein-biased) where adverse central and peripheral responses were observed with this ligand **(Supplementary Table 8).**

We next took advantage of an earlier finding from our laboratory that the bitopic nature of GSK1034702 binding to M1 mAChR meant that GSK1034702 acted as an agonist at both wild type M1 mAChR and M1-DREADD receptors (see; [10])**.** This meant that this ligand could uniquely be used as an agonist in wild type mice, as well as M1-DREADD and M1-DREADD PD mice. Administration of GSK1034702 at a dose that had no adverse effects in M1-DREADD mice (30 mg/kg) had profound peripheral and central adverse effects in M1-DREADD PD mice **(Supplementary**

Table 9), a result consistent with the notion that M1 mAChR signal transduction that is biased toward G protein coupling results in adverse central and peripheral cholinergic responses.

Discussion

In this study we generated a series of novel chemogenetic and G protein-bias mouse models that not only revealed the importance of phosphorylation/arrestin dependent signalling in M1 mAChR-mediated learning and memory and anxiolytic behaviours but also established that the phosphorylation status of the M1 mAChR significantly contributes to minimising cholinergic adverse effects. These adverse effects, both peripheral SLUDGE effects (**s**alivation, **l**acrimation, **u**rination, **d**efecation, **g**astro-intestinal disturbance and **e**mesis) and central adverse responses, such as seizures, have represented one of the major barriers to the success of targeting muscarinic receptors in AD[30,35]. Furthermore, our data suggest that in addition to pro-cognitive benefits, targeting the M1 mAChR in AD might also have an impact on associated behavioural abnormalities including anxiety and hyper-activity.

By uniquely employing DREADD-knockin mice we not only mimic the pharmacological activation of M1 mAChRs but also reveal something of the nature of acetylcholine neuro-signalling since it would appear that cholingeric tone, disrupted in AD, can be mimicked by pharmacological agents allowing for *"normal"* neuronal activity and behavioural responses in a background where cholinergic transmission has been compromised.

In this study we wanted to determine the potential of employing the concept of biased ligands in directing M1 mAChR signalling to therapeutically beneficial pathways by mapping those responses that lie downstream of G protein-dependent versus phosphorylation/arrestin pathways (summarised in Fig 4M). To do this we generated a G protein biased M1 mAChR by deleting all the potential phospho-acceptor sites**.** Interestingly, removal of these phosphorylation sites reduced, but did not eliminate, the interaction of the receptor with arrestin. This is in contrast to other

GPCR subtypes where removal of phosphorylation sites results in almost complete absence of receptor/arrestin interaction (e.g. ref[36]). GPCRs can interact with arrestins via both a phosphorylation-dependent interaction with the *phospho-sensor* and via interaction with the *activation sensor*[37]. Structural studies are revealing the molecular basis for this bimodal binding[38,39], in particular the role of differential phosphorylation patterns driving different arrestin conformations and signalling outputs[40,41] - supporting the hypothesis of a phosphorylation barcode [42,43]. Here we report that the interaction of the M1 mAChR with arrestin, similar to that previously reported for the M3 mAChR [23,44,45], is only partially dependent on the phosphorylation status of the receptor indicating that the *activation sensor* on arrestin plays an equally important role as the *phosphorylation sensor* for the interaction of the M1 mAChR with arrestin. This may be significant when interpreting the phenotypic data of the M1-PD mice since the phenotypes identified here as dependent on the phosphorylation status of the M1 mAChR might not necessarily be due to a deficiency in receptor/arrestin interaction. Rather it is possible that receptor-phosphorylation is important for the correct assembly/activity of M1 mAChR signalling complexes in neurons in a manner that is independent of arrestin.

Classically, phosphorylation of GPCRs is related to receptor desensitisation [46,47]. Hence, one explanation for the phenotypes observed in the M1-PD mice might be that the receptor is unable to undergo phosphorylation-dependent desensitisation. That this might be the case was illustrated by the examination of the locomotion response. In agreement with previous studies [22,48], we demonstrate that M1-KO mice are hyper-active, indicating a role for the M1 mAChR in reducing locomotion. However, M1-PD mice are hypo-active**,** a result that might be interpreted to mean

that the phosphorylation-deficient receptor itself is over-active due possibly to a lack of desensitisation.

However, when we assess the coupling of the phosphorylation-deficient receptor to G protein signalling in membranes and cortical slices from tissues derived from M1-PD mice we see only a very small increase in coupling to G protein signalling. Furthermore, salivary secretion, which we show here is downstream of G protein coupling is not significantly affected in the M1-PD mice. These data point to the intriguing possibility that some physiological responses mediated by G protein signalling are desensitised by receptor phosphorylation (e.g. locomotion) whilst others (e.g. salivary secretion) are not.

The impact of biased signalling on cholinergic adverse responses was strikingly revealed in a set of experiments employing a G protein-biased M1-DREADD mutant mouse. In this mouse line we found that administration of CNO, at concentrations that caused no adverse responses in wild type or M1-DREADD mice, resulted in profound peripheral and central adverse responses, including seizures. Whereas it is clear from previous studies that adverse responses might be related to the degree of efficacy of muscarinic ligands (including the extent of co-operativity and intrinsic activity of PAMs) [7,15] there has not been any previous indication that receptor phosphorylation-dependent processes might have a role in regulating adverse responses. Given our data it might be anticipated that ligands showing signalling bias away from receptor phosphorylation pathways and towards G protein coupling might show more pronounced cholinergic adverse responses. This was found to be the case with pilocarpine, which we show here to be both G protein biased and possessing pronounced seizurogenic activity (consistent with previous studies[31-33]). In contrast, GSK1034702, which was not biased, showed no seizures when

administered to WT mice at a dose that gave the same receptor occupancy as pilocarpine. Interestingly, GSK1034702 only induced cholinergic adverse responses in phosphorylation-deficient, G protein-biased, mice (i.e. M1-PD and M1-DREADD PD). These data point to muscarinic ligands with a bias toward receptor phosphorylation-dependent signalling as having a lower propensity to mediating adverse responses.

Our study adds to a growing body of evidence that M1 mAChRs can be responsible for peripheral adverse effects previously thought to be mediated by M2/M3 receptors[27,29,49]. Hence, simply developing highly selective M1 mAChR agonists might not be sufficient to avert cholinergic side effects. This conclusion is supported by reports that selective M1 mAChR PAMs also display adverse cholinergic responses[7,14,15]. These adverse events appear to be linked with intrinsic activity since those PAMs possessing high agonist activity also show cholinergic adverse responses[7,14,15] whilst those PAMs devoid of intrinsic agonist activity induce no cholinergic toxicity [7,50]. What is not clear, and a point that certainly deserves further investigation, is whether PAMs that possess high agonist activity and significant adverse responses are also biased toward G protein signalling. That this may be the case is supported by data where those PAMs inducing adverse responses (e.g. PF-06767832 and PF-06827443) also stimulate robust inositol phosphate signalling (indicative of Gq-signalling) in striatal tissue [14,29].

Given these studies, and taking into consideration our findings, we conclude that to minimise cholinergic side effects whilst delivering maximal clinical efficacy across a range of AD symptoms next generation M1 mAChR ligands should, in addition to being highly selective and have carefully calibrated efficacy, also drive receptor phosphorylation-dependent signalling.

Acknowledgements

This work is funded by a University of Glasgow Lord Kelvin Adam Smith Fellowship (SJB); an MRC MICA, MR/P019366/1 (ABT, SJB, MR, CM); a Wellcome Trust Collaborative Award, 201529/Z/16/Z (ABT, PV, AC, LD, CM, PMS); SULSA Dementia Seed Funding (ABT, PV, SS); ARUK, PPG2017B-005 (SS) and an MRC iCASE studentship with Eli Lilly (MS). This work was also supported by an MRC group leader programme awarded to ABT at the MRC Toxicology Unit. We acknowledge the BSU facilities at the Cancer Research UK Beatson Institute (C596/A17196) and the Biological Services at the University of Glasgow. Thanks also to Maria Gaellman for the support to the Tobin laboratory.

Author contributions

SJB and ABT devised the programme of work and wrote the paper with assistance from all other authors; SJB, ABT, RAJC, LMB, EMR, SS, PMS, AJM and AC designed and advised on experiments; LD conducted receptor phosphorylation studies; CM and LF managed the mouse colony and conducted mouse behavioural experiments with SJB; PV, CW and LF conducted the EEG recording studies; MS, MR, RM conducted signalling and internalisation studies; KAS, EC, VNB conducted *in vivo* receptor occupancy and *in vivo* ligand activity assays and KG and DAS conducted arrestin assays.

Competing Financial Interests

The authors declare that there are no competing financial interests

References

1 Bartus, R. T., Dean, R. L., 3rd, Beer, B. & Lippa, A. S. The cholinergic hypothesis of geriatric memory dysfunction. *Science* **217**, 408-414 (1982).

2 Courtney, C. *et al.* Long-term donepezil treatment in 565 patients with Alzheimer's disease (AD2000): randomised double-blind trial. *Lancet* **363**, 2105-2115, doi:10.1016/S0140-6736(04)16499-4 (2004).

3 Inglis, F. The tolerability and safety of cholinesterase inhibitors in the treatment of dementia. *Int J Clin Pract Suppl*, 45-63 (2002).

4 Bradley, S. J. *et al.* M1 muscarinic allosteric modulators slow prion neurodegeneration and restore memory loss. *The Journal of clinical investigation* **127**, 487-499, doi:10.1172/JCI87526 (2017).

5 Digby, G. J. *et al.* Novel allosteric agonists of M1 muscarinic acetylcholine receptors induce brain region-specific responses that correspond with behavioral effects in animal models. *J Neurosci* **32**, 8532-8544, doi:32/25/8532 [pii]
10.1523/JNEUROSCI.0337-12.2012 (2012).

6 Ghoshal, A. *et al.* Potentiation of M1 Muscarinic Receptor Reverses Plasticity Deficits and Negative and Cognitive Symptoms in a Schizophrenia Mouse Model. *Neuropsychopharmacology* **41**, 598-610, doi:10.1038/npp.2015.189 (2016).

7 Moran, S. P. *et al.* M1-positive allosteric modulators lacking agonist activity provide the optimal profile for enhancing cognition. *Neuropsychopharmacology*, doi:10.1038/s41386-018-0033-9 (2018).

8 Shirey, J. K. *et al.* A selective allosteric potentiator of the M1 muscarinic acetylcholine receptor increases activity of medial prefrontal cortical neurons and restores impairments in reversal learning. *J Neurosci* **29**, 14271-14286, doi:29/45/14271 [pii]
10.1523/JNEUROSCI.3930-09.2009 (2009).

9 Bodick, N. C. *et al.* Effects of xanomeline, a selective muscarinic receptor agonist, on cognitive function and behavioral symptoms in Alzheimer disease. *Archives of neurology* **54**, 465-473 (1997).

10 Bradley, S. J. *et al.* Bitopic Binding Mode of an M1 Muscarinic Acetylcholine Receptor Agonist Associated with Adverse Clinical Trial Outcomes. *Mol Pharmacol* **93**, 645-656, doi:10.1124/mol.118.111872 (2018).

11 Budzik, B. *et al.* Novel N-Substituted Benzimidazolones as Potent, Selective, CNS-Penetrant, and Orally Active M1 mAChR Agonists. *ACS medicinal chemistry letters* **1**, 244-248, doi:10.1021/ml100105x (2010).

12 Nathan, P. J. *et al.* The potent M1 receptor allosteric agonist GSK1034702 improves episodic memory in humans in the nicotine abstinence model of cognitive dysfunction. *The international journal of neuropsychopharmacology / official scientific journal of the Collegium Internationale Neuropsychopharmacologicum* **16**, 721-731, doi:10.1017/S1461145712000752 (2013).

13 Conn, P. J., Christopoulos, A. & Lindsley, C. W. Allosteric modulators of GPCRs: a novel approach for the treatment of CNS disorders. *Nat Rev Drug Discov* **8**, 41-54, doi:nrd2760 [pii]
10.1038/nrd2760 (2009).

14 Davoren, J. E. *et al.* Design and Synthesis of gamma- and delta-Lactam M1 Positive Allosteric Modulators (PAMs): Convulsion and Cholinergic Toxicity of an M1-Selective

PAM with Weak Agonist Activity. *Journal of medicinal chemistry* **60**, 6649-6663, doi:10.1021/acs.jmedchem.7b00597 (2017).

15 Rook, J. M. *et al.* Diverse Effects on M1 Signaling and Adverse Effect Liability within a Series of M1 Ago-PAMs. *ACS chemical neuroscience* **8**, 866-883, doi:10.1021/acschemneuro.6b00429 (2017).

16 Nickols, H. H. & Conn, P. J. Development of allosteric modulators of GPCRs for treatment of CNS disorders. *Neurobiol Dis* **61**, 55-71, doi:10.1016/j.nbd.2013.09.013 (2014).

17 Smith, J. S., Lefkowitz, R. J. & Rajagopal, S. Biased signalling: from simple switches to allosteric microprocessors. *Nat Rev Drug Discov* **17**, 243-260, doi:10.1038/nrd.2017.229 (2018).

18 Marlo, J. E. *et al.* Discovery and characterization of novel allosteric potentiators of M1 muscarinic receptors reveals multiple modes of activity. *Mol Pharmacol* **75**, 577-588, doi:10.1124/mol.108.052886 (2009).

19 Armbruster, B. N., Li, X., Pausch, M. H., Herlitze, S. & Roth, B. L. Evolving the lock to fit the key to create a family of G protein-coupled receptors potently activated by an inert ligand. *Proc Natl Acad Sci U S A* **104**, 5163-5168, doi:0700293104 [pii]
10.1073/pnas.0700293104 (2007).

20 Roth, B. L. DREADDs for Neuroscientists. *Neuron* **89**, 683-694, doi:10.1016/j.neuron.2016.01.040 (2016).

21 Thompson, K. J. *et al.* DREADD Agonist 21 Is an Effective Agonist for Muscarinic-Based DREADDs in Vitro and in Vivo. *ACS Pharmacol Transl Sci* **1**, 61-72, doi:10.1021/acsptsci.8b00012 (2018).

22 Gerber, D. J. *et al.* Hyperactivity, elevated dopaminergic transmission, and response to amphetamine in M1 muscarinic acetylcholine receptor-deficient mice. *Proc Natl Acad Sci U S A* **98**, 15312-15317, doi:10.1073/pnas.261583798 (2001).

23 Bradley, S. J. *et al.* Mapping physiological G protein-coupled receptor signaling pathways reveals a role for receptor phosphorylation in airway contraction. *Proc Natl Acad Sci U S A* **113**, 4524-4529, doi:10.1073/pnas.1521706113 (2016).

24 Reiter, E. & Lefkowitz, R. J. GRKs and beta-arrestins: roles in receptor silencing, trafficking and signaling. *Trends Endocrinol Metab* **17**, 159-165, doi:S1043-2760(06)00056-7 [pii]
10.1016/j.tem.2006.03.008 (2006).

25 Butcher, A. J. *et al.* An antibody biosensor establishes the activation of the M1 muscarinic acetylcholine receptor during learning and memory. *J Biol Chem*, doi:10.1074/jbc.M115.681726 (2016).

26 Gautam, D. *et al.* Cholinergic stimulation of salivary secretion studied with M1 and M3 muscarinic receptor single- and double-knockout mice. *Mol Pharmacol* **66**, 260-267, doi:10.1124/mol.66.2.260 (2004).

27 Alt, A. *et al.* Evidence for Classical Cholinergic Toxicity Associated with Selective Activation of M1 Muscarinic Receptors. *J Pharmacol Exp Ther* **356**, 293-304, doi:10.1124/jpet.115.226910 (2016).

28 Bodick, N. C. *et al.* The selective muscarinic agonist xanomeline improves both the cognitive deficits and behavioral symptoms of Alzheimer disease. *Alzheimer Dis Assoc Disord* **11 Suppl 4**, S16-22 (1997).

29 Davoren, J. E. *et al.* Discovery of the Potent and Selective M1 PAM-Agonist N-[(3R,4S)-3-Hydroxytetrahydro-2H-pyran-4-yl]-5-methyl-4-[4-(1,3-thiazol-4-yl)ben

zyl]pyridine-2-carboxamide (PF-06767832): Evaluation of Efficacy and Cholinergic Side Effects. *Journal of medicinal chemistry* **59**, 6313-6328, doi:10.1021/acs.jmedchem.6b00544 (2016).

30 Felder, C. C. *et al.* Current status of muscarinic M1 and M4 receptors as drug targets for neurodegenerative diseases. *Neuropharmacology* **136**, 449-458, doi:10.1016/j.neuropharm.2018.01.028 (2018).

31 Cavalheiro, E. A., Santos, N. F. & Priel, M. R. The pilocarpine model of epilepsy in mice. *Epilepsia* **37**, 1015-1019 (1996).

32 Levesque, M., Avoli, M. & Bernard, C. Animal models of temporal lobe epilepsy following systemic chemoconvulsant administration. *J Neurosci Methods* **260**, 45-52, doi:10.1016/j.jneumeth.2015.03.009 (2016).

33 Turski, W. A. *et al.* Limbic seizures produced by pilocarpine in rats: behavioural, electroencephalographic and neuropathological study. *Behav Brain Res* **9**, 315-335 (1983).

34 Mogg, A. J. *et al.* In vitro pharmacological characterization and in vivo validation of LSN3172176 a novel M1 selective muscarinic receptor agonist tracer molecule for positron emission tomography (PET). *J Pharmacol Exp Ther*, doi:10.1124/jpet.117.246454 (2018).

35 Bender, A. M., Jones, C. K. & Lindsley, C. W. Classics in Chemical Neuroscience: Xanomeline. *ACS chemical neuroscience* **8**, 435-443, doi:10.1021/acschemneuro.7b00001 (2017).

36 Prihandoko, R. *et al.* Distinct Phosphorylation Clusters Determine the Signaling Outcome of Free Fatty Acid Receptor 4/G Protein-Coupled Receptor 120. *Mol Pharmacol* **89**, 505-520, doi:10.1124/mol.115.101949 (2016).

37 Gurevich, V. V. & Gurevich, E. V. The structural basis of arrestin-mediated regulation of G-protein-coupled receptors. *Pharmacol Ther* **110**, 465-502, doi:10.1016/j.pharmthera.2005.09.008 (2006).

38 Shukla, A. K. *et al.* Structure of active beta-arrestin-1 bound to a G-protein-coupled receptor phosphopeptide. *Nature* **497**, 137-141, doi:10.1038/nature12120 (2013).

39 Zhou, X. E. *et al.* Identification of Phosphorylation Codes for Arrestin Recruitment by G Protein-Coupled Receptors. *Cell* **170**, 457-469 e413, doi:10.1016/j.cell.2017.07.002 (2017).

40 Mayer, D. *et al.* Distinct G protein-coupled receptor phosphorylation motifs modulate arrestin affinity and activation and global conformation. *Nat Commun* **10**, 1261, doi:10.1038/s41467-019-09204-y (2019).

41 Staus, D. P. *et al.* Sortase ligation enables homogeneous GPCR phosphorylation to reveal diversity in beta-arrestin coupling. *Proc Natl Acad Sci U S A* **115**, 3834-3839, doi:10.1073/pnas.1722336115 (2018).

42 Butcher, A. J. *et al.* Differential G-protein-coupled receptor phosphorylation provides evidence for a signaling bar code. *J Biol Chem* **286**, 11506-11518, doi:M110.154526 [pii]
10.1074/jbc.M110.154526 (2011).

43 Nobles, K. N. *et al.* Distinct phosphorylation sites on the beta(2)-adrenergic receptor establish a barcode that encodes differential functions of beta-arrestin. *Science signaling* **4**, ra51, doi:10.1126/scisignal.2001707 (2011).

44 Kong, K. C. *et al.* M3-muscarinic receptor promotes insulin release via receptor phosphorylation/arrestin-dependent activation of protein kinase D1. *Proc Natl Acad Sci U S A* **107**, 21181-21186, doi:1011651107 [pii]
10.1073/pnas.1011651107 (2010).
45 Poulin, B. *et al.* The M3-muscarinic receptor regulates learning and memory in a receptor phosphorylation/arrestin-dependent manner. *Proc Natl Acad Sci U S A* **107**, 9440-9445, doi:0914801107 [pii]
10.1073/pnas.0914801107 (2010).
46 Lefkowitz, R. J. A brief history of G-protein coupled receptors (Nobel Lecture). *Angewandte Chemie* **52**, 6366-6378, doi:10.1002/anie.201301924 (2013).
47 Lefkowitz, R. J. Historical review: a brief history and personal retrospective of seven-transmembrane receptors. *Trends Pharmacol Sci* **25**, 413-422 (2004).
48 Miyakawa, T., Yamada, M., Duttaroy, A. & Wess, J. Hyperactivity and intact hippocampus-dependent learning in mice lacking the M1 muscarinic acetylcholine receptor. *J Neurosci* **21**, 5239-5250, doi:21/14/5239 [pii] (2001).
49 Kurimoto, E. *et al.* An Approach to Discovering Novel Muscarinic M1 Receptor Positive Allosteric Modulators with Potent Cognitive Improvement and Minimized Gastrointestinal Dysfunction. *J Pharmacol Exp Ther* **364**, 28-37, doi:10.1124/jpet.117.243774 (2018).
50 Rook, J. M. *et al.* A Novel M1 PAM VU0486846 Exerts Efficacy in Cognition Models without Displaying Agonist Activity or Cholinergic Toxicity. *ACS chemical neuroscience* **9**, 2274-2285, doi:10.1021/acschemneuro.8b00131 (2018).

Figure Legends

Figure 1: Generation of the M1-DREADD knock-in mouse

(A) Snake-plot of the M1 receptor identifying the mutations introduced to generate the M1-DREADD receptor. **(B)** Quantitative RT-PCR showing the transcription of M1 mAChR RNA in the hippocampus or cortex of wild type (WT) or M1-DREADD mice. Data are expressed as a ratio of β-actin RNA transcription (n=3 mice). **(C, D)** Solubilised membranes prepared from the hippocampus **(C)** or cortex **(D)** of WT, M1-HA, M1-DREADD and M1-KO mice were probed in Western blot analysis for the expression of M1 mAChR using an antibody for the HA tag. Data shown are two separate mice for each genotype, with similar data being obtained on at least two further occasions *(see; figS2)*. Na^+/K^+ATPase expression was used as a loading control. **(E, F)** Stimulation of [^{35}S]-GTPγS binding to cortical membranes prepared from WT, M1-HA **(E)** or M1-DREADD **(F)** mice following stimulation with carbachol (CCh) or clozapine-*n*-oxide (CNO). Data are expressed as means ± S.E.M. of 3-4 independent experiments performed in duplicate and normalized to the maximal response at the WT receptor.

Figure 2: Altered phenotypes of M1-DREADD mice are corrected by CNO

(A-F) Heat maps showing the occupancy of wild type (WT) **(A, D)**, M1-KO **(B, E)** and M1-DREADD **(C, F)** mice in the elevated plus maze (EPM) test following administration of vehicle **(A-C)** or 0.3 mg/kg CNO **(D-F)** (i.p. 30 min prior to test). Heat maps represent the occupancy (Blue = 0 sec occupancy, red = 5 sec occupancy) of 2-6 mice per treatment group. **(G)** Mean anxiety level of WT, M1-KO or M1-DREADD mice treated with vehicle or CNO (calculated as a ratio of open/closed arm entries divided by the total number of entries) prior to the EPM test.

Data represent 16-26 individual mice, and were analysed using a two-way ANOVA with a Sidak's multiple comparison test (*P<0.05, **P<0.01, ***P<0.001).

(H-J) Representative motion plots of wild type (WT) **(H)**, M1-KO **(I)** or M1-DREADD **(J)** mice in the open field test. **(K)** Average distance travelled by WT, M1-KO or M1-DREADD mice over a 10 min period in the open field test (inset total distance for each genotype over a 10 min period). Data are means of 3-5 separate mice. **(L)** Total distance travelled in an 8 min period by WT, M1-KO or M1-DREADD following administration of vehicle or 0.3 mg/kg CNO 30 min prior to a Y maze test. Data are means ± S.E.M. of 4-13 individual mice, and were analysed using a two-way ANOVA with a Sidak's multiple comparison test (**P<0.01; ***P<0.001).

Figure 3: Generation of the G protein biased M1-PD knock-in mouse

(A) Snake-plot of the M1 receptor identifying the mutations introduced to generate the M1-PD receptor. **(B)** Stimulation of intracellular Ca^{2+} release in HEK cells transiently transfected with mouse M1-WT or M1-PD mAChRs. **(C)** β-arrestin recruitment to the M1 mAChR determined using PathHunter HEK cells expressing either the M1 WT or M1-PD receptor. Shown are concentration response curves to the full muscarinic receptor agonist oxotremorine-M (oxo-M). The data are the means ± S.E.M. of three independent experiments and are expressed as a percentage of the maximal response to Oxo-M at the wild type (WT) M1 mAChR. **(D)** Representative images showing the localisation of HA-tagged M1 WT or M1-PD in CHO cells stimulated with vehicle or 100 μM carbachol for 1 hour prior to fixation with 4% PFA (63x objective). Data shown are representative of 4 individual experiments. **(E)** [^{3}H]-NMS binding to cortical membranes prepared from WT M1-HA or M1-PD mice (n=4). Data shown are the means ± S.E.M. **(F)** Quantitative RT-PCR

showing the transcription of M1 mAChR RNA in the hippocampus or cortex of WT and M1-PD mice. Data are expressed as a ratio of β-actin RNA transcription (n=3 mice). **(G, H)** Solubilised membranes prepared from the hippocampus **(G)** or cortex **(H)** of WT M1-HA, M1-PD and M1-KO mice were probed in Western blot analysis for the expression of M1 mAChR using an antibody for the HA tag. Data shown are two separate mice for each genotype, with similar data being obtained on at least two further occasions *(see; fig S6).* Na^+K^+ATPase expression was used as a loading control. **(I, J)** Stimulation of [^{35}S]-GTPγS $G_{q/11}$ binding **(I)** or Ins(1,4,5)P_3 accumulation **(J)** in cortical tissue prepared from WT M1-HA or M1-PD mice following stimulation with CCh. Data are expressed as means ± S.E.M. of 3 independent experiments performed in duplicate ([^{35}S]-GTPγS) or triplicate (Ins(1,4,5)P_3 accumulation) and normalized to the maximal response at the WT receptor.

Figure 4: Mapping of bimodal signalling to M1 mAChR physiological responses

(A-C) Heat maps showing the occupancy of wild type (WT) (n=13), M1-PD (n=14) or M1-KO (n=4) mice in the open- or closed arms of the EPM (blue = 0 sec occupancy, red = 5 sec occupancy). **(D)** Anxiety level of WT (n=21), M1-KO (n=15) or M1=PD (n=14) mice (calculated as a ratio of open/closed arm entries divided by the total number of entries). **(E)** Total distance travelled in the EPM of WT (n=13), M1 PD (n=14) or M1-KO (n=15). Data shown are means ± S.E.M. and were analysed using a one-way ANOVA with Dunnett's multiple comparisons test; *P<0.05; ***P<0.001. **(F)** WT or M1-PD mice were tested for 8 min in a Y maze spontaneous alternation paradigm to assess spatial working memory. Data shown are means ± S.E.M. and

were analysed using a Student's t test (*P<0.05). **(G-I)** Representative track plots of WT, M1-DREADD and M1-KO mice in the open field (OF) test. **(J)** Total distance travelled in a 10 min period by WT, M1-PD and M1-KO mice during an OF test. Data shown are means ± S.E.M. and were analysed using a one-way ANOVA with Dunnett's multiple comparisons test; *P<0.05. **(K)** Basal locomotor activity of WT M1-HA, M1-PD and M1-KO mice was assessed using *in vivo* telemetry recordings. Mean locomotor activity ± S.E.M. of 8 mice over a 24 hour period is shown, with total locomotor activity during this period calculated by measurement of the area under the curve (AUC). **(L)** Salivary secretion in response to pilocarpine (1 mg/kg) administration was measured in WT, M1-PD and M1-KO mice. The data represent the means ± S.E.M. of n=5-7 mice. Data were analysed using a one-way ANOVA with Dunnett's multiple comparisons test compared to WT mice; *P<0.05. **(M)** An illustration of the M1 mAChR physiological responses lying downstream of G protein-dependent signalling (saliva secretion and locomotion) versus phosphorylation-dependent signalling (anxiolytic behaviour and spatial working memory).

Figure 5: M1-DREADD PD mice show epileptic-like seizures

(A) Snake-plot of the M1 mAChR identifying the mutations introduced to generate the M1-DREADD PD receptor. **(B)** Quantitative RT-PCR showing the transcription of M1 mAChR RNA in the hippocampus or cortex of wild type (WT), M1-DREADD or M1-DREADD PD mice. Data are expressed as a ratio of β-actin RNA transcription (n=3 mice). **(C, D)** Solubilised membranes prepared from the hippocampus **(C)** or cortex **(D)** of WT M1-HA, M1-DREADD, M1-DREADD PD and M1-KO mice were probed in Western blot analysis for the expression of M1 mAChR using an antibody for the HA tag. Data shown are two separate mice for each genotype, with similar

data being obtained on at least two further occasions *(see; fig S2)*. Na^+K^+ATPase expression was used as a loading control. **(E-F)** Stimulation of [^{35}S]-GTPγS binding to cortical membranes prepared from M1-DREADD **(E)** or M1-DREADD PD **(F)** mice following stimulation with CCh or CNO. Data are expressed as means ± S.E.M. of 3-4 independent experiments performed in duplicate and normalized to the maximal response at the WT receptor. **(G)** Raw cortical EEG signals (top) and the spectrogram (bottom) in a representative M1-DREADD PD mouse following administration of CNO (0.3 mg/kg; i.p.) after 15 min of recording basal cortical activity. **(H)** Normalized EEG power in M1-DREADD or M1-DREADD PD mice treated with vehicle (5% glucose) or CNO (0.3 mg/kg). Data shown are means ± S.E.M. of 4-8 individual mice and were analysed using a repeated measures ANOVA, $F(3, 3119) = 5.53$, $p = 0.029$.

Figure 6: Pilocarpine shows G protein bias, whilst GSK1034702 is not biased

Inositol phosphate (IP_1) accumulation **(A)**, ERK1/2 phosphorylation (pERK) **(B)** or M1 mAChR phosphorylation at Serine 228 (pSer228) **(C)** stimulated by acetylcholine (ACh), pilocarpine or GSK1034702 in CHO cells stably expressing the mouse wild type M1 mAChR. Dashed line shows data generated as part of a previous dataset for comparison (see; ref [10]). **(D)** Preferential signalling bias ($(\Delta\Delta Log_{10}(\tau/K_A))$) stimulated by ACh, pilocarpine and GSK1034702 towards IP_1, pERK or pSer228 pathways at the WT M1 receptor is shown. Data are means ± S.E.M. and used ACh as the reference ligand. **(E, F)** Stimulation of inositol phosphate accumulation in the frontal cortex of male Sprague Dawley rats followed by administration of increasing concentrations of GSK1034702 **(E)** or pilocarpine **(F)**. Data shown are means ± S.E.M. of 3-4 rats and were analysed using a two-way ANOVA with Dunnett's

multiple comparison, where *P<0.05, **P<0.01 versus vehicle, and $^{\#}P$<0.05, $^{\#\#}P$<0.01 versus LiCl.

Online Materials

Animal maintenance

All mice were bred as homozygous onto a C57BL/6J background. Male and female animals at 8–12 weeks old were used if not stated otherwise. Mice were fed ad libitum with a standard mouse chow and were maintained within the animal facility at least 1 week prior to experiments. Animals were cared for in accordance with national guidelines on animal experimentation. All experiments were performed under a project license from the British Home Office (United Kingdom) under the Animals (Scientific Procedures) Act of 1986.

Generation of M1-PD, M1-DREADD, M1-DREADD PD knock-in animals

For the generation of the knock-in animals a construct containing the loxP-Stop-loxP cassette upstream of a sequence encoding for the M1-HA, M1-PD, M1-DREADD or M1-DREADD PD was generated and inserted within the encoding exon (exon 3) of the M1 mAChR gene (*Chmr1*). All constructs were tagged with a HA epitope sequence (YPYDVPDYA) appended to the C terminus. The M1-DREADD is the coding sequence for the humanized (humanizing mutations V5A, S254T, K320R, G337A, and V413I) M1 mAChR with two mutations Y106C and A196C **(see; Fig 1A).** The M1-PD is the coding sequence of the mouse M1 mAChR with mutations in the third intracellular loop and C-terminal tail that replace 20 serine resides with alanine **(see; Fig 4A).** The M1-DREADD PD is the coding sequence for the humanized M1-DREADD plus 20 serine-alanine mutations in the third intracellular loop and C-terminal tail **(see; Fig 6A)**.

The targeting vectors containing the coding sequences for the muscarinic receptor mutants were subsequently transfected into **embryonic stem (ES) cells derived**

from C57BL/6J mice and neomycin-resistant ES cells were selected. Homologous recombination was validated by PCR and southern blot. Recombined ES cell clones were injected into blastocysts for the generation of chimeric mice. Breeding of chimeras with C57BL/6 and Cre-recombinase expressing mice allowed the generation of heterozygous mice. Heterozygous animals were bred for the generation of homozygous lines. M1-KO mice were conditional M1-PD mice expressing a Stop of transcription cassette flanked with loxP sites upstream of the M1-PD cDNA. To obtain these mice please contact the corresponding authors. The generation of M1-HA, M1-PD, M1-DREADD, M1-DREADD PD and M1-KO mice was carried out by genOway.

Note that the M1-KO strain was generated using conditional M1-PD mice that were not crossed with any CRE-deleter strains therefore leaving the stop cassette upstream of the ATG intact resulting in a mouse strain where the receptor was not expressed **(see; the summary of the construct Fig S4).**

qRT-PCR

RNA was isolated from hippocampus or cortex of WT, M1-DREADD, M1-DREADD PD, M1-PD or M1-KO mice using Qiagen lipid tissue RNeasy kit as per manufacturer instructions. RNA concentration was quantified using a Nanodrop and 1 µg total RNA template per reaction was used for cDNA synthesis using SuperScript III first-strand synthesis SuperMix (Invitrogen). RNA/water (total 8 µl), 2 µl RT enzyme and 10 µl 2x RT reaction mix were mixed together and incubated for 10 min at 25°C, followed by 30 min at 50°C, followed by 5 min at 85°C. Samples were then chilled on ice. Each reaction was performed in the presence and absence of RT enzyme (- RT

control). Finally, cDNA was incubated with 1 µl (2U) of E. Coli RNAse H and at 37°C for 20 min and subsequently stored at -20°C until qRT-PCR was performed.

For qRT-PCR, the following M1 mAChR primers were used (at 300:300 dilution):

F: 5' CAAGTGGCATTCATCGGGATCACC

R: 5' GAGAAAGTGCCAATGATGAGATCAGC

Each reaction was performed in triplicate. Each reaction was performed in a total volume of 25 µl containing: 12.5 µl SYBR Green Master Mix, 0.75 µl F primer (10 µM stock), 0.75 µl R primer (10 µM stock), 10 µl water and 1 µl cDNA (or –RT sample).

IP1 accumulation assay

Human M1-WT or M1-DREADD PD constructs were stably expressed in CHO-FlpIn cells and grown to confluence in T75cm^2 flasks in Ham's F-12 media containing 10% fetal bovine serum and 1% penicillin/streptomycin and under hygromycin B selection (400 µg/ml). Cells were harvested and centrifuged at 1000 xg for 3 min prior to resuspension in 1X stimulation buffer ((in mM): HEPEs, 10; $CaCl_2$, 1; $MgCl_2$, 0.5; KCl, 4.2; NaCl, 146; glucose, 5.5; LiCl, 50; pH7.4) at 1.43 x 10^6 cells/ml. Test compounds (7 µl/well) and cell suspension (7 µl/well) were added to 384-well white proxiplates (PerkinElmer). Following a brief centrifugation, plates were incubated at 37°C for 45 min. The IP1-d2 conjugate and the anti-IP1 cryptate Tb conjugate (IP1 Tb™ assay kit, CisBio) were diluted 1:30 in lysis buffer and 3 µl of each were added to each well. The plate was incubated at 37°C for 1h and FRET between d2-conjugated IP1 (emission at 665 nm) and Lumi4™-Tb cryptate conjugated anti-IP1 antibody (emission at 620 nm) was detected using an Envision plate reader (PerkinElmer). Results were calculated from the 665/620 nm ratio and normalised to the maximum response stimulated by ACh.

ERK1/2 phosphorylation

Stimulation of ERK1/2 phosphorylation (Thr 202/Tyr 204) was assessed using the CisBio Phospho-ERK Cellular Assay Kit. Confluent monolayers of CHO Flp-In cells stably expressing the human M1 mAChR were serum starved overnight prior to the experiment. Cells were washed with 100 µl phosphate-buffered saline and incubated in serum free F12 medium at 37°C. Cells were stimulated with test compounds for 5 min at 37°C in a final volume of 200 µl. The stimulations were terminated by rapid aspiration and addition of 50 µl lysis buffer supplemented with blocking reagent. Lysates were gently agitated at room temperature for 30 min. Subsequently, 16 µl of this lysate was transferred to a 384-well white ProxiPlate (PerkinElmer) and incubated with 4 µl premixed antibody solution for 2 hours at room temperature. Fluorescence emission (665 and 620 nm) was determined using a PHERAstar plate reader (BMG Labtech).

Cell culture and transfection (for Ca^{2+} and β-arrestin recruitment assays)

PathHunter™ HEK293:β-arrestin:EA cells were transfected with the mouse WT or the mouse phosphorylation-deficient M1 mAChR in the ProLink vector (DiscoverX, UK), and grown under antibiotic selection (G418) to produce a stable pool of cells expressing the receptor. HEK293 wt/pdM_1:β-arrestin:EA cells were maintained in DMEM medium containing L-glutamine supplemented with foetal bovine serum (FBS; 10 % v/v), hygromycin B (250 µg ml^{-1}) geneticin G418 (500 ug ml^{-1}) at 37°C, 5% CO_2.

Intracellular Ca^{2+} measurement

PathHunter™ HEK293 wt/pdM_1:β-arrestin cells were seeded into 96-well clear bottom, black plates (Costar) at 40,000 cells/well in 90 µl cell culture medium and incubated at 37 °C, 5 % CO_2 overnight to achieve a confluent monolayer. On the day of the experiment, 30 µL of 4x Ca^{2+} no-wash assay kit 4 (Molecular Devices) containing 0.02 % pluronic acid (1:1); 2.5 mM probenecid, was added to each well of the 96-well cell plate and incubate at 37°C, 5 % CO_2 for 30 min. Agonist-induced changes in $Ca^{2+}{}_i$ concentration were then monitored over time using a FlexStation 3 (Molecular Devices, UK). Basal fluorescence was monitored for 16 s prior to addition of a range of M_1 mACh receptor agonists, after which changes in fluorescence recorded for a further 60 sec. Responses to agonist were expressed as change in fluorescence from baseline to peak. The maximum fluorescence was taken as the highest point of the initial peak following agonist addition. The minimum fluorescence was taken as the background fluorescence prior to agonist addition.

Arrestin recruitment assay

PathHunter™ HEK293 wt/pdM_1:β-arrestin cells cells were seeded overnight in white, clear bottom 384-well ViewPlates (PerkinElmer, UK) at 8,000 cells/well in 20 µl cell culture medium and incubated at 37°C, 5 % CO_2 overnight to achieve a confluent monolayer. On the day of the assay, spent medium was removed and replaced with HBSS containing 0.1 % BSA (w/v) and 20 mM HEPES, at pH 7.4. Cells were stimulated with a range of M_1 mACh receptor agonists for 2 hr (in 5 µL), after which time 25 µL or proprietary Flash detection reagent (DiscoveRx, UK) was added and plate incubated for 15 min at room temperature in the dark. Luminescence was read on the ClarioStar (BMG, UK) using the Luminescent protocol, no filter.

Western Blotting

Preparation of membrane extracts

Membrane extracts were prepared following a protocol similar to the membrane preparation described by[1]. Briefly, hippocampi were homogenised by sonication at 3-5 µg amplitude in 25 mM sodium phosphate buffer, pH 7.4, and containing proteinase inhibitors. Samples are then centrifuged at 20,000 xg for 30 min at 4 °C. The pellets were then incubated with 1.2 % digitonin in 25 mM sodium phosphate and 5 mM $MgCl_2$ buffer (pH 7.4) overnight at 4°C with end over end rotation. After centrifugation of samples at 20,000 xg for 30 min at 4°C, the supernatants (membrane extracts) were transferred to fresh microcentrifuge tubes and stored at -80°C until use. Protein concentrations were determined by using the Micro BCA protein assay reagent kit according to the manufacturer's instructions.

Western blotting analysis

Samples were incubated with Laemmli loading buffer containing 5% β-mercaptoethanol for 30 min at 37°C and loaded in 7.5% SDS-Tris-glycine polyacrylamide gels. Samples were run at ±100 V following the transfer onto nitrocellulose membranes that were blocked for 2 h with 5% fat free milk in TBS-T (0.1% tween-20 in TBS at pH 7.4). Membranes were then incubated with the respective primary antibody overnight at 4°C, then washed three times with TBS-T (10 min each wash) and incubated with the respective secondary antibody (1:5000) conjugated to horseradish peroxidase. Proteins were visualised with the ECL detection system (signal westpico plus chemiluminsescent substrate #34578).

[^{3}H]-NMS binding

Membrane preparations of mouse hippocampus or cortex (50 µg/tube) were incubated in binding buffer (in mM: HEPEs, 50; NaCl, 110; KCl, 5.4; $CaCl_2$, 1.8; $MgSO_4$, 1; glucose, 25; sucrose, 58; pH 7.4) containing increasing concentrations (0.1 - 5 nM) of [^{3}H]-*N*-methyl scopolamine ([^{3}H]-NMS) for 1 hour at 37°C. Membrane-bound ligand was separated from free ligand by rapid filtration onto GF/B glass microfiber filters followed by three washes with ice-cold 0.9% NaCl. Membrane bound radioactivity was determined by liquid scintillation (Perkin Elmer Ultima Gold) counting. Nonspecific binding was determined in the presence of atropine (1 µM) during the incubation with [^{3}H]-NMS.

[^{35}S]-GTPγS assay

M1-WT, M1-DREADD, M1-PD and M1-DREADD PD (8-12 weeks) were humanely killed and cortical tissue was dissected on ice. Tissue was suspended in ice-cold buffer A (containing 0.9% (w/v) NaCl, 10 mM HEPES, 0.2% (w/v) EDTA, pH 7.4) and homogenised (4 x 5 sec bursts) using a Polytron homogeniser. The suspension was centrifuged at 200 xg for 5 min at 4°C using an Eppendorf 5810R bench-top centrifuge. Supernatants were collected and re-homogenised as above. The suspension was subsequently centrifuged for 20 min at 40,000 xg at 4°C using a Beckman Coulter Avanti JXN-26 centrifuge with a JA-25.25 rotor. Supernatant was discarded, and the pellet was re-suspended in 10 mL ice-cold buffer B (10 mM HEPES, 10 mM EDTA, pH 7.4). The pellet was homogenised, GTP (1 mM final) was added and the suspension was incubated at 37°C for 15 min. The suspension was subsequently centrifuged for 20 min at 40,000 xg at 4°C and the pellet was re-suspended in 15 mL ice-cold buffer C (10 mM HEPES, 0.1 mM EDTA, pH 7.4) and re-homogenised as before. Suspension was centrifuged again for 20 min at 40,000

xg at 4°C. The final pellet was re-suspended in buffer C and protein concentration was estimated using a Bradford assay. The homogenate was then further diluted in final storage buffer to produce a concentration of 2 mg/ml.

[^{35}S]-GTPγS binding and immunoprecipitation of Gα subunits was performed as previously described [1] . Specifically, M1-WT, M1-DREADD, M1-PD or M1-DREADD PD membranes were diluted in assay buffer (in mM: HEPES, 10; NaCl, 100; $MgCl_2$, 10; pH 7.4) containing a final concentration of 1 μM GDP. Membranes (75 μg in a total assay volume of 200 μL) were added to [^{35}S]-GTPγS (1 nM final concentration) and agonists (CCh or CNO) and incubated at 30°C for 5 min. Reactions were terminated by the addition of 1 mL ice-cold assay buffer and immediate transfer to an ice bath. Samples were centrifuged (20,000 xg, 6 min, 4°C) and membrane pellets solubilised by the addition of 50 μL ice-cold solubilisation buffer (100 mM Tris HCl, 200 mM NaCl, 1 mM EDTA, 1.25% Igepal and 0.2% SDS, pH 7.4) and incubation for 1 h at 4°C on a shaking platform. Following complete protein re-solubilisation, 50 μL of solubilisation buffer without SDS was added. Solubilised protein was pre-cleared using normal rabbit serum at a dilution of 1:100 and 3% (w/v) protein A-sepharose beads in TE buffer (10 mM Tris HCl, 10 mM EDTA, pH 8.0) added for 60 min at 4°C. Protein A- sepharose beads and insoluble material were collected by centrifugation (20,000 xg, 6 min, 4°C) and 100 μL of the supernatant was transferred to fresh tubes containing Gq-specific anti-serum (Santa Cruz; sc393) and incubated overnight at 4°C. Protein A-sepharose beads were added to samples, vortex mixed and rotated at 4°C for 90 min before being centrifuged (10,000 xg, 1 min, 4°C). Supernatants were aspirated and the protein A- sepharose beads washed three times with ice-cold solubilisation buffer (without SDS). Recovered beads were then mixed with 1 mL FloScint-IV scintillation cocktail and counted by liquid scintillation spectrometry.

Ins(1,4,5)P_3 mass assay

M1-HA or M1-PD mice were humanely killed via cervical dislocation. The brain was exposed transferred to an ice-cold platter and cerebral cortex dissected. Cerebral cortex was cross-chopped using a McIlwain tissue chopper (300 µm x 300 µm). The resulting tissue cubes were dispersed into Krebs-Henseleit buffer (KHB (in mM): NaCl, 118; KCl, 4.7; $MgSO_4$, 1.2; $NaHCO_3$, 25; NaH_2PO_4, 1.2; $CaCl_2$, 1.3; HEPES, 10; glucose, 11; pH 7.4 after equilibration with O_2/CO_2 95:5), washed by multiple buffer changes and then shaken in an oscillating water bath for 60 min at 37^{o}C; tissue cubes were sedimented under gravity and buffer changed every 10 min during this period.

At the end of the washing period cerebral cortex cubes were allowed to sediment under gravity and 25 µL aliquots of 'packed' tissue transferred to a flat-bottomed 5 mL tube containing 250 µL KHB. Each tube was purged with O_2/CO_2 (95:5), capped and returned to a shaking water bath at 37^{o}C. Drug additions were made (bringing the total incubation volume to 300 µL), tubes again purged with O_2/CO_2 (95:5) and incubations continued for the times indicated in figure legends. Incubations were terminated by addition of an equal volume of ice-cold 1 M trichloroacetic acid and tubes allowed to extract on ice for 30 min. Tubes were then centrifuged (2,000 xg, 20 min, 4^{o}C). Supernatants were recovered, neutralised using the dichlorodifluoromethane/tri-*n*-octylamine method and inositol 1,4,5-trisphosphate (IP_3) concentration was determined exactly as described previously[2]. Tissue cube pellets were solubilized by addition of 1 M NaOH. Protein concentration was

determined for each incubation using the Lowry method. This allowed IP_3 mass accumulation to be expressed as pmol IP_3 mg^{-1} protein.

Elevated plus maze

The mice were habituated to the EPM testing room overnight and were maintained in the dark until testing. Where mice received vehicle (5% glucose) or CNO (0.3 mg/kg), this was administered 30 min prior to the test via intraperitoneal (i.p.) injection.

The elevated plus maze (EPM) consisted of four non-transparent arms (50 x 10cm); two enclosed arms (with black walls of 30cm height), and two dimly illuminated open arms. Mice were placed into the centre of the elevated plus maze, facing the closed arm. Mice were tracked using ANY-maze software for 5 min, and the number of entries into the closed or open arms during this time was monitored. Anxiety level was calculated as a percentage of open arm entries versus total entries made. The maze was cleaned with 70% ethanol between each animal.

Open field

General locomotor activity was assessed using the open field test, following overnight habituation in the behavioural testing suite. Mice were placed into a clear, Perspex square arena (50 x 50 cm) and activity was tracked for a 10 min period using ANY-maze software.

Y maze

Mice were habituated to the behavioural testing suite overnight prior to the test. For tests where mice received vehicle (5% glucose) or CNO (0.3 mg/kg), these were administered via i.p. injection 30 min prior to the start of the test. Mice were placed into the centre of a Y maze (grey, non reflective base plate) with three identical arms (A, B, C; lane width: 5 cm; arm length: 35 cm; arm height: 10cm). Activity was recorded using ANY-maze software. Spontaneous alternation behaviour was calculated by measuring the number of "ABC" sequences (in any order) as a proportion of the total triplet sequences made during the 8 min test.

***In vivo* telemetry**

The basal locomotor activity was measured in intact freely moving WT, M1-PD and M1-KO mice by telemetric system (Data Sciences International, St Paul, MN, USA). The TA-F10 implantable probes (1.1 cc; 1.6 grams) were implanted in the peritoneal cavity under the isoflurane (1.5-2%) anaesthesia and carprofen (Rimadyl®; 5 mg/kg s.c.) analgesia. During the implantation, the mice were kept on the thermostable pad. After the surgery, mice were housed individually and left 1 week for recovery before being used in the experiment. Basal locomotor activity was acquired directly from the transponders for three consecutive days during which the animals were not disturbed. Locomotor activity was recorded in home cages. Receivers were connected through MX2 matrix directly to the PC into a single computer port, allowing for the determination of all parameters. The data were collected every 60 sec and Ponemah® acquisition system (DSI) was used for collecting and first processing of data.

Biorhythm analysis

The data from telemetry experiment collected by Ponemah® acquisition system (DSI) were grouped into 10 min sequences, and the calculated means were used for further analysis. The analysis was performed using the ChronosFit program[3] employing Fourier analysis and the stepwise regression technique.

EEG recordings

Surgery and recording

Animals (M1-HA WT, M1-DREADD, M1-MDREADD PD) were anesthetised with isoflurane (1–1.5%) and placed in a stereotaxic frame (model SR-5M-HT; Narishige, Japan). Animals' head were shaved using electric clippers and cleaned with ethanol (70%) and iodopovidone. Lidocaine (2%, 0.1–0.3 mg) was administered subcutaneously at the site of incision and carprofen (Rimadyl®; 5 mg/kg) was administered subcutaneously to provide analgesia after the surgery. The body temperature of animals was maintained at 37°C using a heating pad during the entire surgery. Five bone screws were fixed in the skull, two in the frontal region (AP +1.5 mm, ML ± 1 mm from bregma) used as electrodes for frontal cortical electroencephalograms (EEGs), two in the parietal region (AP - 2 mm, ML ± 2 mm from bregma) used for parietal cortical EEGs and one on the cerebellum as a ground and a reference. Then the electrodes with screws were attached with dental cement as a head-post. After the head-post surgery the animals were left to recover for at least 5 days before using in the experiment. During an acclimation period of 5 days, the animals were on daily basis handled, placed in recording chamber and the animal's head was tethered to the recording cable. The following day after the acclimation period, the animals were placed back in the recording chamber for electrophysiological recording.

The recording was performed as followed. The initial 15 min served for the recording of basal cortical activity. Then, mice were injected (i.p.) with vehicle (5% glucose) or with CNO (0.3 mg/kg) and EEGs recording continued for another 45 (75) min. During the whole experimental procedure, mice were allowed to freely move and were monitored for the occurrence of seizures.

After animals were anesthetised with isoflurane (1 - 1.5%), they were placed in a stereotaxic frame (SR-5M-HT, Narishige) and body temperature was retained at 37°C using a feedback temperature controller (50-7221-F, Harvard Bioscience, Inc.). Lidocaine (2%, 0.1 ml) was administered subcutaneously at the site of incision and Carprofen (Rimadyl, 5 mg/kg) was also administered subcutaneously at the back. After incision, the skull was exposed and cleaned. Four bone screws were implanted and used for cortical electroencephalogram (EEG) recording. Another screw was implanted over the cerebellum as a ground and a reference. All screws were connected with a connector and covered with dental cement. The animals were left to recover for at least 5 days.

Electrophysiological recording procedures are described elsewhere [3-4] Briefly, the animal was placed in an open box (21.5 cm x 47 cm x 20 cm) by connecting a 16-channel amplifier board (RHD2132, Intan Technologies, LLC) and an interface cable. Signals were amplified relative to a cerebellar bone screw and were digitized at 1000 Hz (RHD2132 and RHD 2000, Intan Technologies, LLC). Each recording session consisted of a 15-min baseline recording, an intraperitoneal injection (CNO, 0.3 mg/kg or vehicle), and another recording for at least 45 min.

All offline analysis was performed using MATLAB (version R2018b, Mathworks). Because all four EEG channels provided qualitatively similar signals, only the signals at the right frontal region were used. To compute spectrogram, the multi-taper spectral estimation method was applied (Chronux Toolbox, http://chronux.org/). To evaluate signal power, root-mean-square (RMS) value was computed in every 1 sec and scaled in dB. After lowpass-filtering the scaled signals at 1/300 Hz, they were normalized relative to the baseline (the mean value of first 5 min signals) to compare them across experiments.

Measurement of saliva secretion

Mice were anesthetised by i.p. injection with 100 mg/kg of ketamine/0.25 mg/kg of medetomidine. Following this procedure, mice were injected with pilocarpine (1 mg/ml, i.p.) and salivary secretion (in milligrams of saliva) onto GF/B filter paper (GE Healthcare Life Sciences) was recorded every 5 min over a 35 min period.

Immunocytochemistry for internalisation of receptors

CHO cells stably expressing HA-tagged (C-terminal) version of the mouse M1-WT, mouse M1-PD, humanized M1-DREADD or humanized M1- DREADD PD were grown for 24 h to achieve 60-80% confluence on 13 mm glass coverslips coated with 0.01% Poly-D-Lysine. Cells were stimulated with 100 μM carbachol (WT and M1-PD) or CNO (M1-DREADD or M1-DREADD PD) for 1 h, fixed using 4% PFA (in TBS buffer), and blocked and permeabilised using 2% BSA in Triton X-100 (0.1% in TBS buffer). Incubation with anti-EEA1 polyclonal antibody (ThermoFisher Scientific; 1:1000) was carried out at 4°C overnight, and incubation with anti-HA antibody (Roche; 1:1000) was performed at room temperature for 2 h. Following three washes

with TBS buffer, secondary antibody incubation with AlexaFluor 594 anti-rabbit and AlexaFluor 488 anti-rabbit (Thermo Fisher; 1:400) was performed for 2 h at room temperature, and followed by three quick washes with TBS. Coverslips with stained cells were mounted on glass slides using VECTASHIELD HardSet Antifade Mounting Medium with DAPI. Data were acquired using a LSM 880 confocal laser scanning microscope (Zeiss).

Rat IP accumulation

Sample Collection

Rat (Sprague-Dawley 250-275g) brain samples (frontal cortex) were collected after animals were administered the following treatments: H_2O vehicle or LiCl (100mg/kg, sc) followed 30 min later by **H_2O** vehicle or scopolamine (1mg/kg, s.c.) or SKF38393 (20 mg/kg, s.c.) at a dose volume of 1 ml/kg. One hour post LiCl administration rats were dosed with pilocarpine (10, 30, or 100 mg/kg, s.c.) or GSK1034702 (3, 10, or 30mg/kg, i.p.). Rats were then sacrificed 2 hours later and frontal cortex collected over dry ice. Samples were stored at -70°C for LC/MS/MS analysis of inositol phosphate.

Mass Spectrometry

Samples were homogenized using a probe sonicator set at level 8 for 10 sec in 5x volumes of 50% acetonitrile containing 0.1% formic acid and 50% methanol (MeOH). Samples were then centrifuged for 12 min at 13000 x g. 100 ul of supernatant was transferred into 200 ul of distilled water and 20ul aliquots of samples were injected onto LC/MS apparatus. Myo-Inositol 2-monophosphate bis (cyclohexylammonium) salt (Sigma Aldrich - I5250) was used to prepare standards (10, 30, 100, 300 and

1000ng/g or ml) in 50% acetonitrile + 50% methanol + 0.1% formic acid). The analysis of inositol phosphate (IP) was carried out using an Agilent 6410 series triple quad LC/MS/MS with MassHunter data analysis software (Agilent Technologies Inc, Santa Clara, CA 95051 U.S.A.) fitted with an electrospray ion source and run in negative mode. Detection was accomplished by monitoring the precursor ion of IP with mass to charge ratio (m/z) of 259 and targeting its product ion with m/z set to 78.9. The chromatographic separation employed a Zorbax RX-SIL HPLC Column, 2.1 X 150mm from (Agilent Technologies Inc, Santa Clara, CA 95051 U.S.A.) and a mobile phase consisting of 3% acetonitrile in water with an overall 0.1% formic acid content with a flow rate of 0.7mL per minute. Clearly delineated chromatographic peaks with the retention time of authentic standards and expected molecular weight were seen after each injection of sample. Analyte were quantified based on the areas of these peaks.

In vivo receptor occupancy

Live Phase

Male Sprague-Dawley rats (N=4 per dose group) were purchased from Harlan (Indianapolis) and ranged in weight from 200-300 g. Pilocarpine or GSK1034702 were administered at doses of 0.03, 0.1, 0.3, 1, 3 and 10 mg/kg for generation of a dose-response. Animals received either vehicle alone (1% Hydroxyethlycellulose, 0.25% Polysorbate 80, 0.05% Antifoam in purified water) or test compound in a dose volume of 10 ml/kg. In the dose response studies, rats received i.v. administration of non-labelled tracer LSN3172176 [5] 10 mg/kg, 0.5 ml/kg dose volume for rats and 5 ml/kg dose volume for mice; in the lateral tail vein 30 min after vehicle or compound administration. Animals were sacrificed by cervical dislocation 20 min after tracer

administration. Brains were removed and dissected. Frontal cortex and cerebellum were used for the tracer measurement and the remaining brain and plasma used for compound exposure analysis. The receptor occupancy is considered to be measured at the time of tracer administration (t). Studies were performed at Covance Alnwick or Greenfield.

Tissue Preparation and Tracer Analysis

Frontal cortex and cerebellar samples were weighed and placed in conical centrifuge tubes on ice. Four volumes (w/v) of acetonitrile containing 0.1% formic acid was added to each tube. Samples were then homogenized using an ultrasonic probe and centrifuged using a bench top centrifuge at 14,000 RPM for 20 min. Supernatant was diluted by adding 50 µL to 150 µL sterile water in 96-well plates for LC/MS/MS analysis. Analysis of LSN3172176 was carried out using an API 4000 mass spectrometer. Chromatographic separation employed an Agilent Zorbax Eclipse XDB-C18 column (2.1 X 50 mm) and a gradient mobile phase consisting of 15% to 90% acetonitrile in water with an overall 0.1% formic acid content. Detection of LSN3172176 was accomplished by monitoring the precursor to product ion transition with a mass to charge ratio (m/z) of 386.3 to 128.0. Standards were prepared by adding known quantities of the tracer to brain tissue samples from non-treated rats or mice and processing as described above.

Receptor Occupancy Determinations

Receptor occupancy was calculated using the ratio method. The level of tracer was measured in each cortical and cerebellar sample. A ratio of cortical levels (total binding) to cerebellar levels (nonspecific binding) was generated for each animal.

Vehicle ratios represent 0% occupancy and a ratio of 1, where the binding in the cortex is equal to the binding in the cerebellum, represents 100% occupancy. The ratios from the pilocarpine and GSK1034702 pretreated groups were interpolated linearly between the ratio in the vehicle-treated animals (0% occupancy) and 1 (100% occupancy) in order to determine the percent M1 receptor occupancy. For the pilocarpine and GSK1034702 dose response, a curve was fitted to a 4-parameter logistic function with the bottom and top fixed at 0% and 100%, respectively using GraphPad Prism version 6.0 and the dose achieving 50% receptor occupancy ($RecOcc_{50}$) was calculated by the software. Values are given as mean ± S.E.M.

For conversion of total plasma or brain levels to unbound levels, the % values for SPP1 free in the plasma (4.4%) and brain (10.1%) were used. The unbound brain to unbound plasma concentration ratio is the KP,uu, where Kp is the total brain to total plasma concentration ratio and uu stands for unbound brain and plasma

Data analysis

Functional concentration-response curves were fitted according to a four-parameter logistic equation (to determine minimum and maximum asymptotes, $LogEC_{50}$, and slope; GraphPad Prism 6). To assess agonist bias, the same concentration-response curves were analyzed according to a modified form of the operational model of agonism, recast to directly yield a transduction ratio ($Log[\tau/K_A]$;[6]): where basal represents the response in the absence of agonist, E_m represents the maximal response of the assay system, K_A represents the equilibrium dissociation constant of the agonist, [A] represents the concentration of agonist, τ is an index of the coupling efficiency (or efficacy) of the agonist, and n is the slope of the transducer function

linking agonist occupancy to response. For the analysis, all families of agonist curves at each pathway were globally fitted to the model with the parameters, basal, E_m, and n shared between all agonists. For full agonists, the $LogK_A$ was constrained to a value of zero, whereas for partial agonists this was directly estimated by the curve fitting procedure; the $Log(\tau/K_A)$ parameter was estimated as a unique measure of activity for each agonist. Agonist bias factors (10^DDLog[τ/K_A]) were calculated as previously described[6].

Data availability statement: All data is available from the authors or is available through the University of Glasgow online data repository

References

1. Bradley, S. J. *et al.* M1 muscarinic allosteric modulators slow prion neurodegeneration and restore memory loss. *The Journal of clinical investigation* **127**, 487-499, doi:10.1172/JCI87526 (2017).Challiss, R. A., Batty, I. H. & Nahorski, S. R. Mass measurements of inositol(1,4,5)trisphosphate in rat cerebral cortex slices using a radioreceptor assay: effects of neurotransmitters and depolarization. *Biochem Biophys Res Commun* **157**, 684-691 (1988).
2. Arraj, M. & Lemmer, B. Circadian rhythms in heart rate, motility, and body temperature of wild-type C57 and eNOS knock-out mice under light-dark, free-run, and after time zone transition. *Chronobiol Int* **23**, 795-812, doi:10.1080/07420520600827111 (2006).
3. Lyngholm, D. & Sakata, S. Cre-Dependent Optogenetic Transgenic Mice Without Early Age-Related Hearing Loss. *Front Aging Neurosci* **11**, 29, doi:10.3389/fnagi.2019.00029 (2019).
4. Yague, J. G., Tsunematsu, T. & Sakata, S. Distinct Temporal Coordination of Spontaneous Population Activity between Basal Forebrain and Auditory Cortex. *Frontiers in neural circuits* **11**, 64, doi:10.3389/fncir.2017.00064 (2017).
5. Mogg, A. J. *et al.* In vitro pharmacological characterization and in vivo validation of LSN3172176 a novel M1 selective muscarinic receptor agonist tracer molecule for positron emission tomography (PET). *J Pharmacol Exp Ther*, doi:10.1124/jpet.117.246454 (2018).
6. van der Westhuizen, E. T., Breton, B., Christopoulos, A. & Bouvier, M. Quantification of ligand bias for clinically relevant beta2-adrenergic receptor ligands: implications for drug taxonomy. *Mol Pharmacol* **85**, 492-509, doi:10.1124/mol.113.088880 (2014).

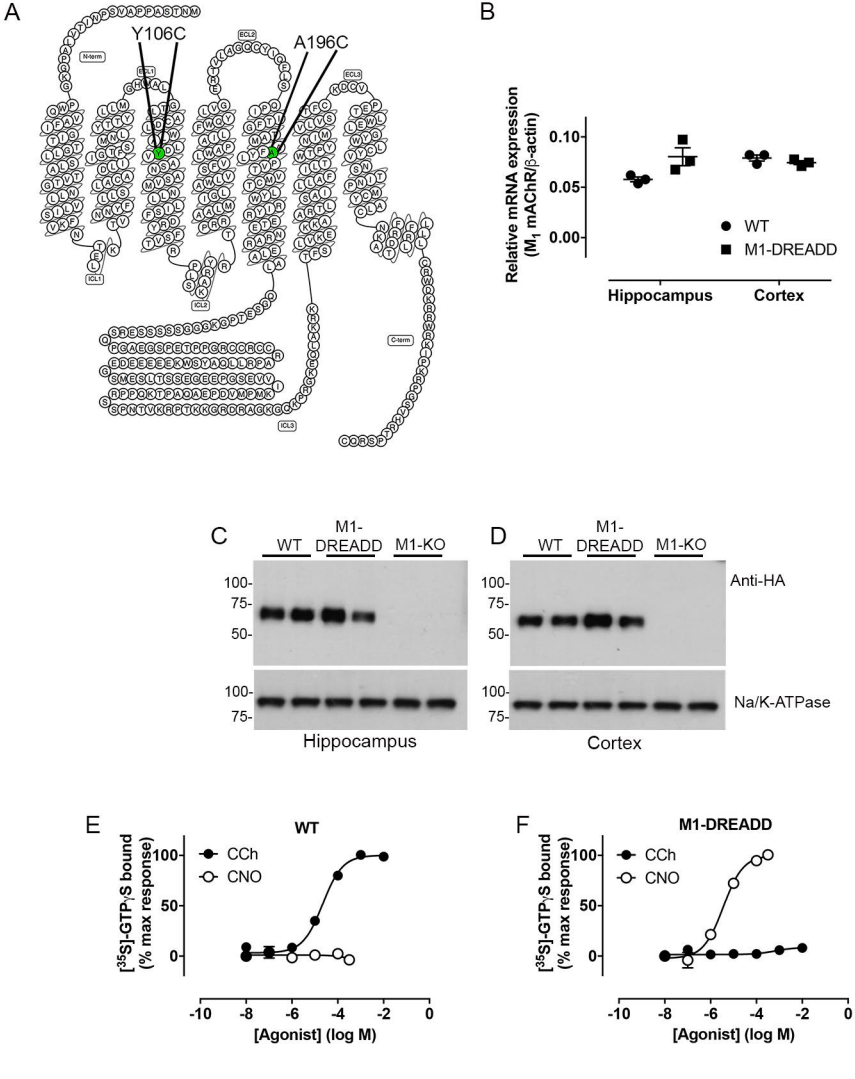
A
Y106C
A196C
N-term
ECL1
ECL2
ECL3
ICL1
ICL2
ICL3
C-term
B
Relative mRNA expression
(M_1 mAChR/β-actin)
0.10
0.05
0.00
WT
M1-DREADD
Hippocampus
Cortex
C
M1-
WT
DREADD
M1-KO
100-
75-
50-
100-
75-
Hippocampus
D
M1-
WT
DREADD
M1-KO
100-
75-
50-
Anti-HA
100-
75-
Na/K-ATPase
Cortex
E
WT
[35S]-GTPγS bound
(% max response)
100
50
0
CCh
CNO
-10
-8
-6
-4
-2
0
[Agonist] (log M)
F
M1-DREADD
[35S]-GTPγS bound
(% max response)
100
50
0
CCh
CNO
-10
-8
-6
-4
-2
[Agonist] (log M)

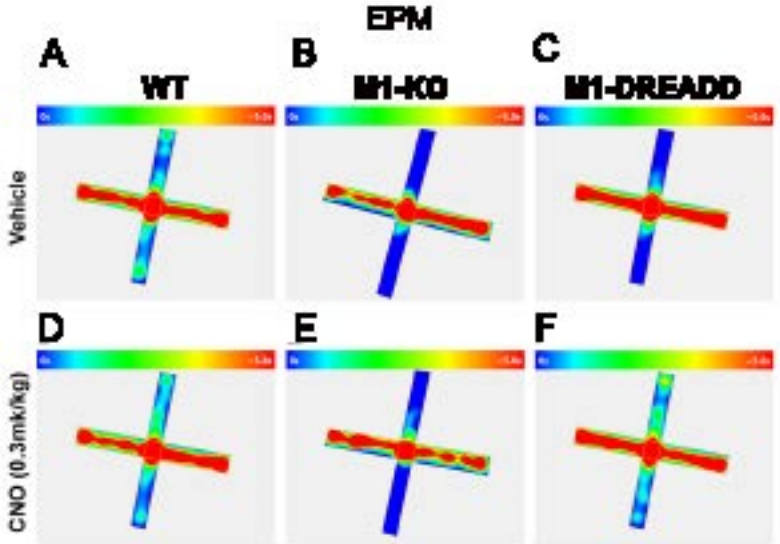
EPM
A
WT
B
M1-KO
C
M1-DREADD
Vehicle
D
E
F
CNO (0.3mk/kg)

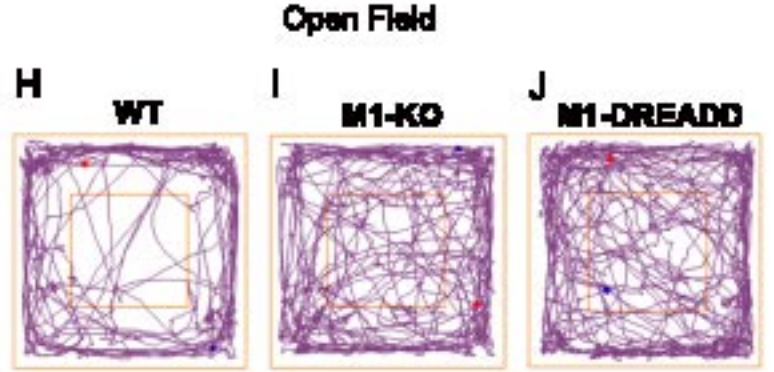
Open Field
H
WT
I
M1-KO
J
M1-DREADD

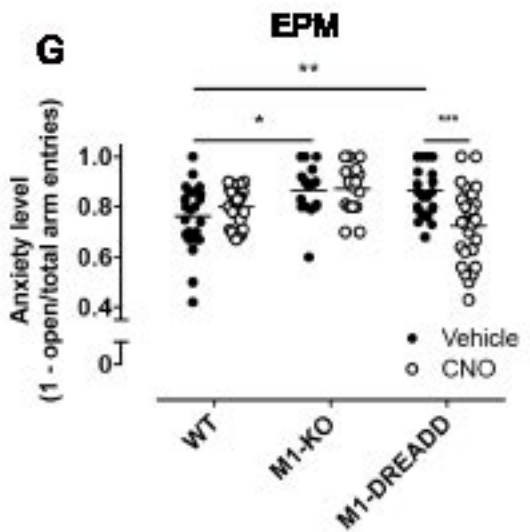
EPM
G
Anxiety level
(1 - open/total arm entries)
1.0
0.8
0.6
0.4
0
Vehicle
CNO
WT
M1-KO
M1-DREADD

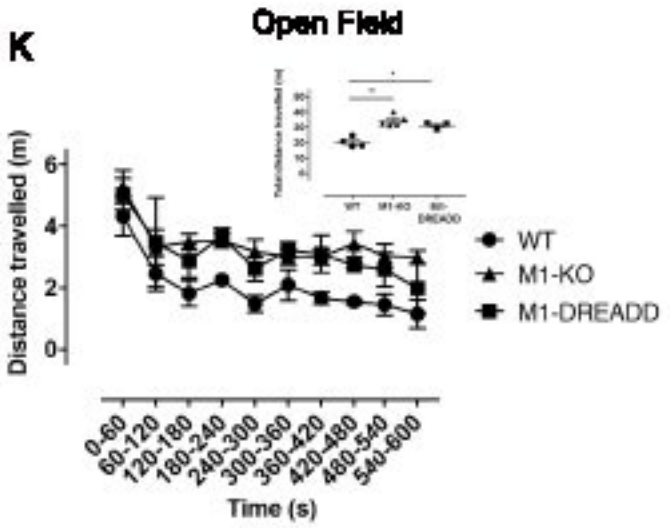
Open Field
K
Distance travelled (m)
6
4
2
0
WT
M1-KO
M1-DREADD
0-60
60-120
120-180
180-240
240-300
300-360
360-420
420-480
480-540
540-600
Time (s)

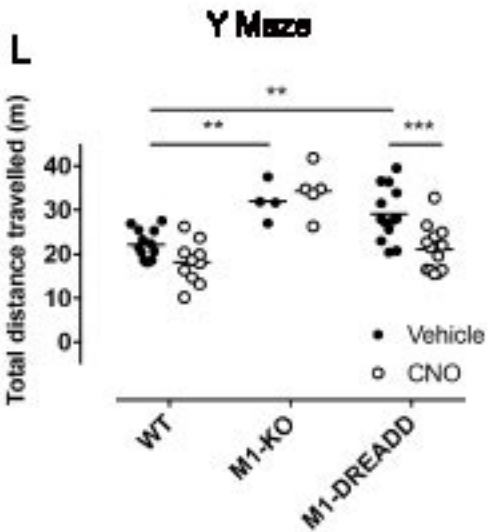
Y Maze
L
Total distance travelled (m)
40
30
20
10
0
Vehicle
CNO
WT
M1-KO
M1-DREADD

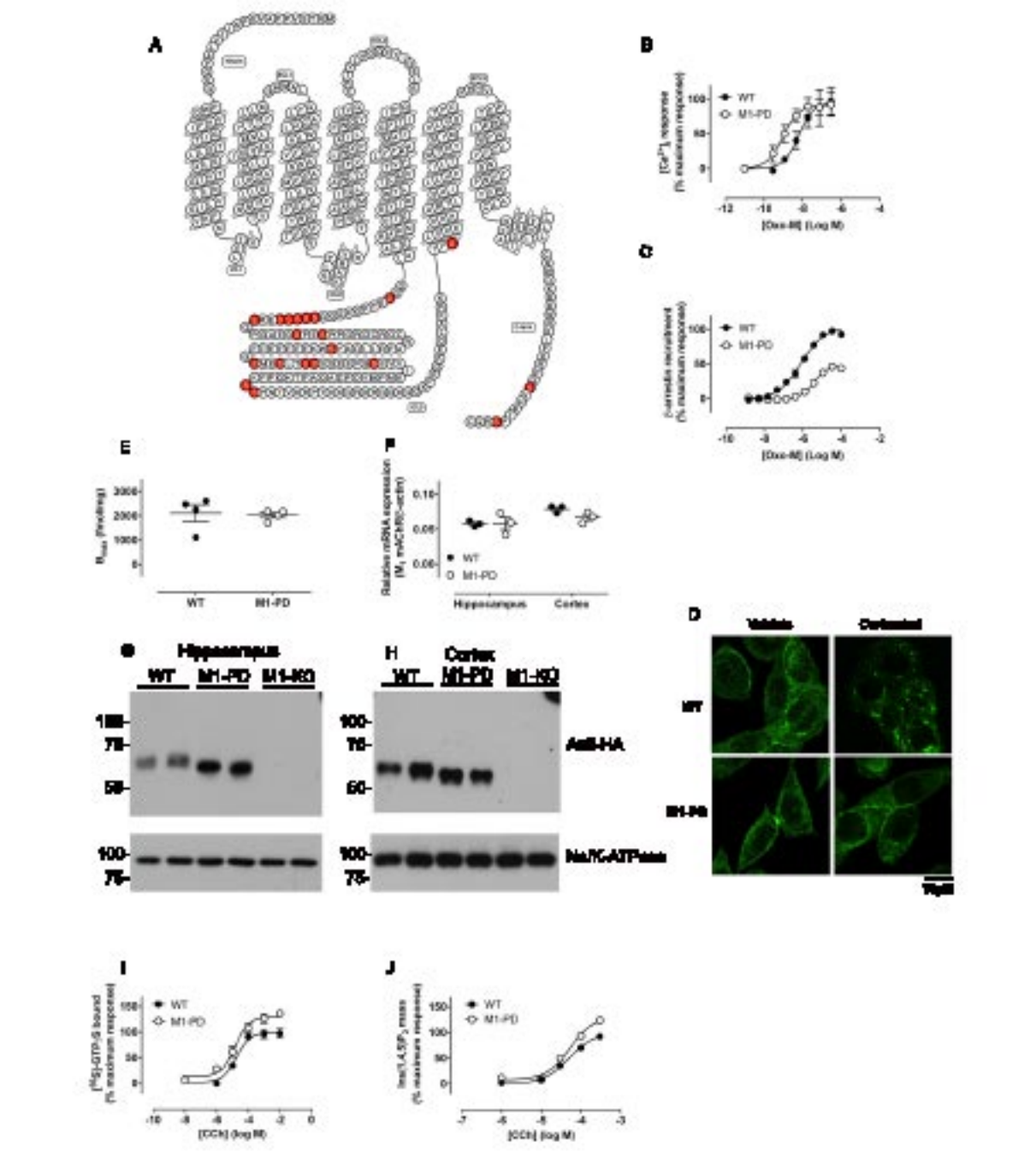
A
B
WT
M1-PD
[Oxo-M] (Log M)
C
WT
M1-PD
[Oxo-M] (Log M)
E
WT
M1-PD
F
WT
M1-PD
Hippocampus
Cortex
G
Hippocampus
WT
M1-PD
M1-KO
AstM1-HA
Na/K-ATPase
H
Cortex
WT
M1-PD
M1-KO
D
Vehicle
Carbachol
WT
M1-PD
I
WT
M1-PD
[CCh] (log M)
J
WT
M1-PD
[CCh] (log M)

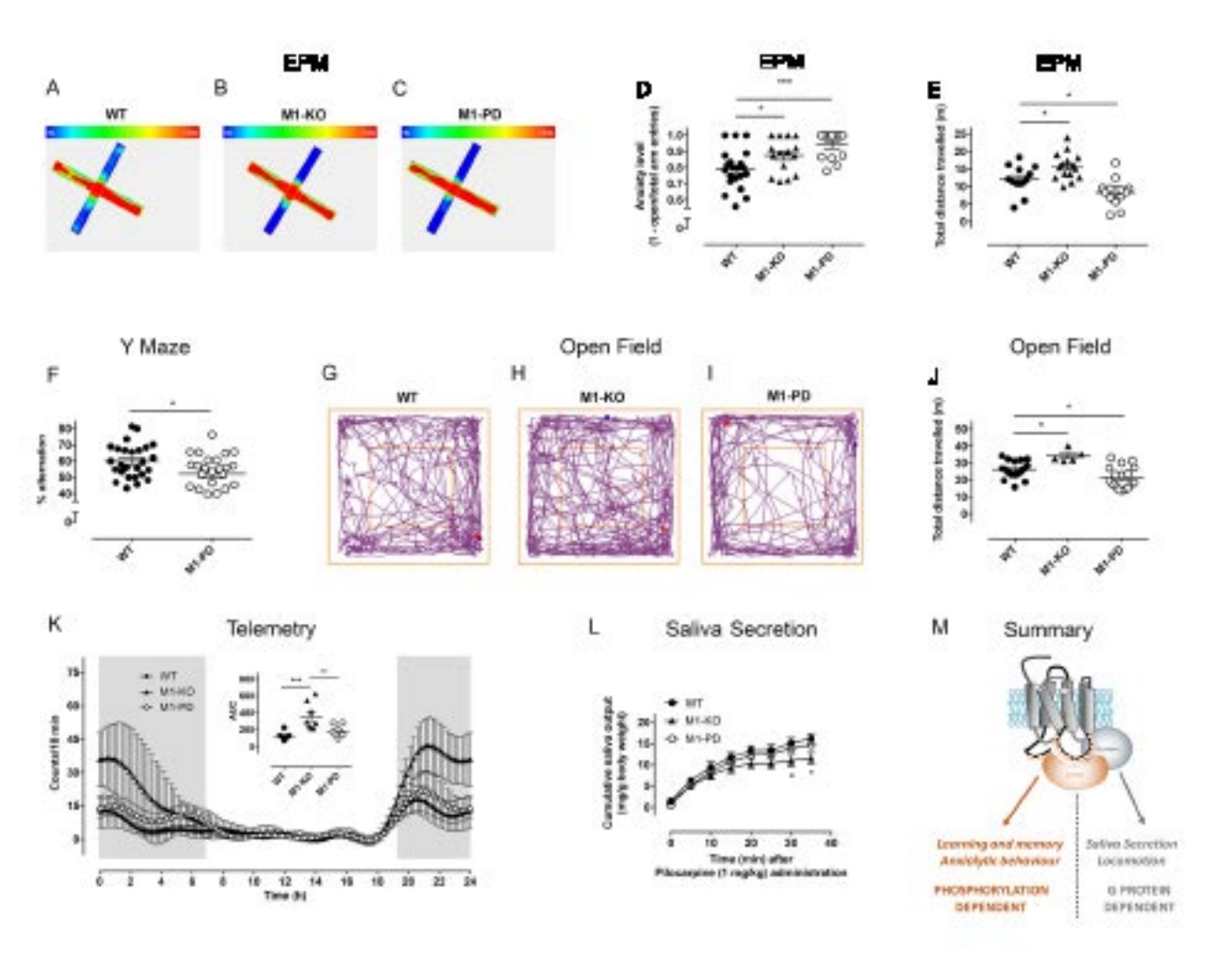
EPM
A
WT
B
M1-KO
C
M1-PD
D
EPM
Anxiety level
(1 - open/total arm entries)
WT
M1-KO
M1-PD
E
EPM
Total distance travelled (m)
WT
M1-KO
M1-PD
Y Maze
F
% alternation
WT
M1-PD
Open Field
G
WT
H
M1-KO
I
M1-PD
Open Field
J
Total distance travelled (m)
WT
M1-KO
M1-PD
K
Telemetry
WT
M1-KO
M1-PD
Counts/10 min
AUC
Time (h)
L
Saliva Secretion
Cumulative saliva output
(mg/g body weight)
WT
M1-KO
M1-PD
Time (min) after
Pilocarpine (1 mg/kg) administration
M
Summary
Learning and memory
Anxiolytic behaviour
PHOSPHORYLATION
DEPENDENT
Saliva Secretion
Locomotion
G PROTEIN
DEPENDENT

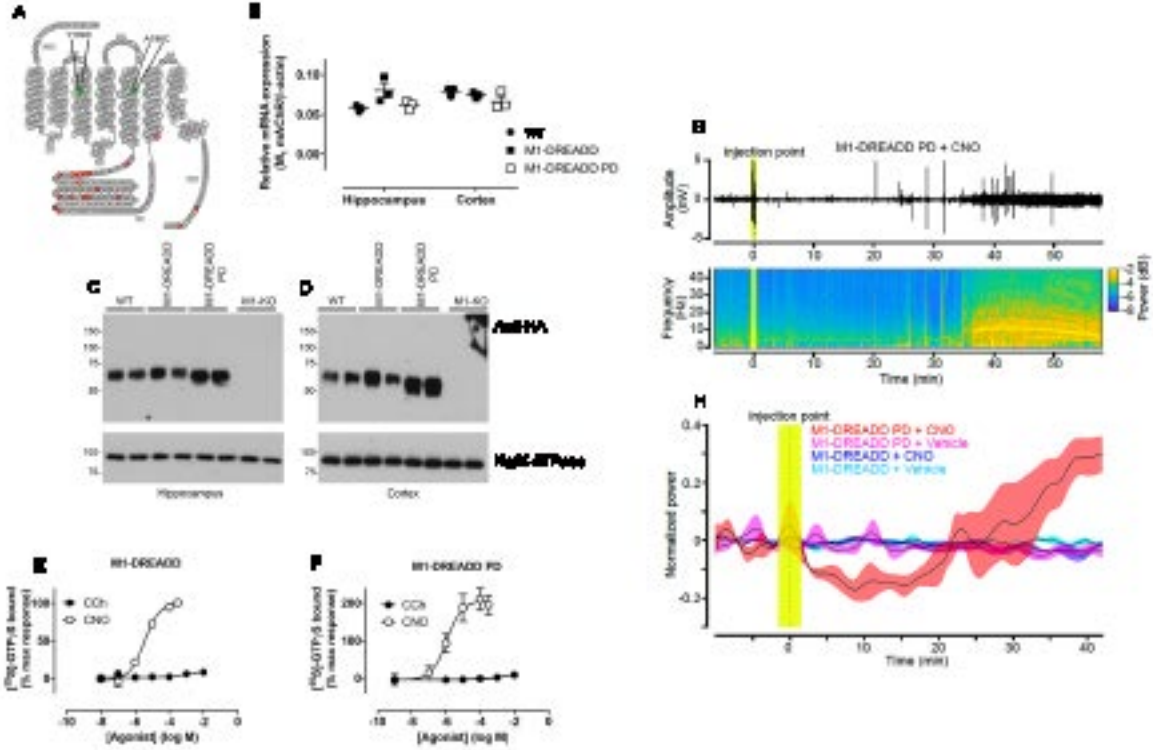
A
B
Relative mRNA expression
WT
M1-DREADD
M1-DREADD PD
Hippocampus
Cortex
C
D
WT
M1-DREADD
M1-DREADD PD
M1-KO
HA
Hippocampus
Cortex
E
M1-DREADD
CCh
CNO
[Agonist] (log M)
F
M1-DREADD PD
CCh
CNO
[Agonist] (log M)
B
Injection point
M1-DREADD PD + CNO
Amplitude
Frequency
Power (dB)
Time (min)
H
Injection point
M1-DREADD PD + CNO
M1-DREADD PD + Vehicle
M1-DREADD + CNO
M1-DREADD + Vehicle
Normalized power
Time (min)

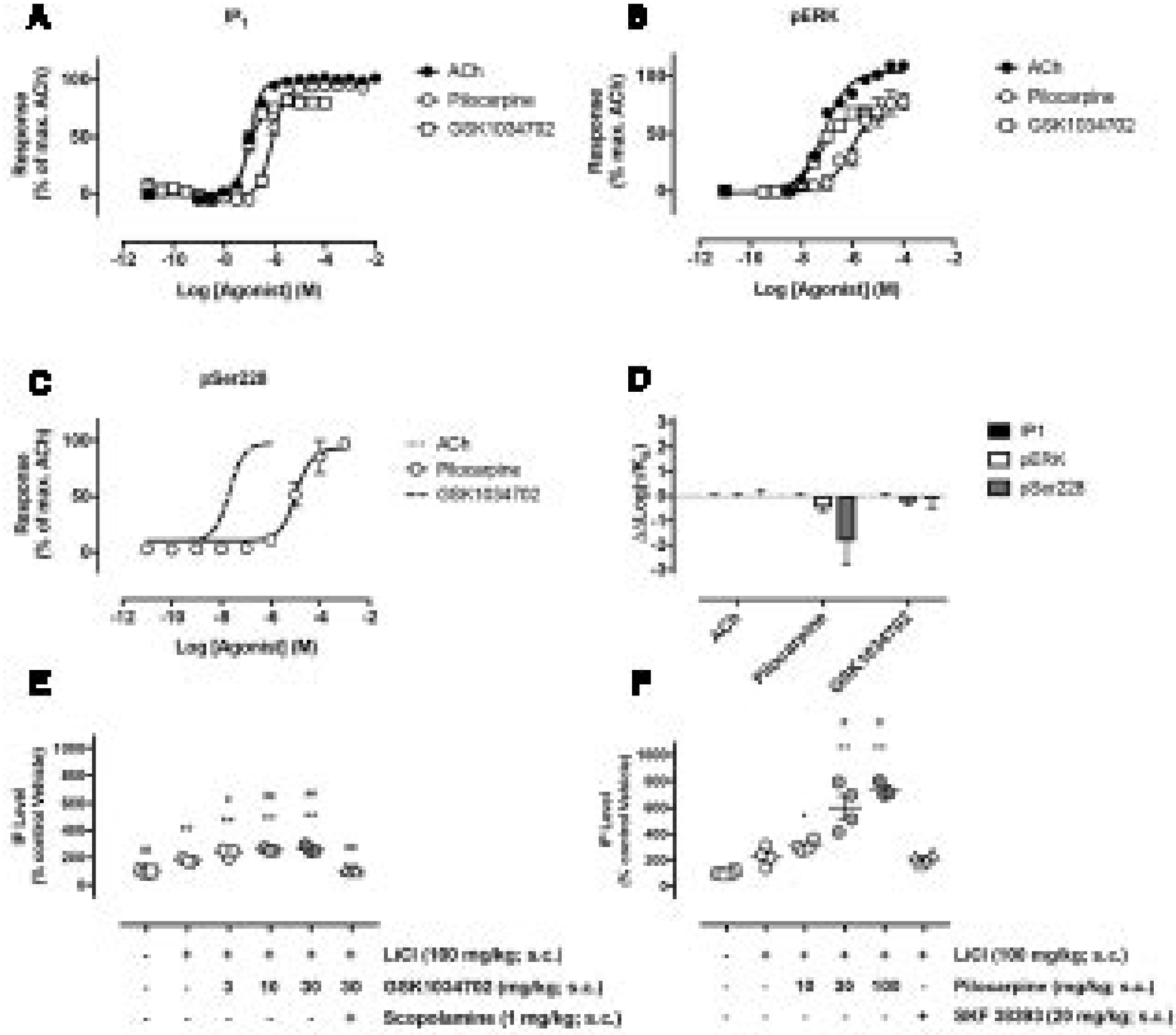
A
IP1
Response (% of max. ACh)
ACh
Pilocarpine
GSK1034702
Log [Agonist] (M)
B
pERK
Response (% max. ACh)
ACh
Pilocarpine
GSK1034702
Log [Agonist] (M)
C
pSer228
Response (% of max. ACh)
ACh
Pilocarpine
GSK1034702
Log [Agonist] (M)
D
IP1
pERK
pSer228
E
IP Level (% control Vehicle)
LiCl (100 mg/kg; s.c.)
GSK1034702 (mg/kg; s.c.)
Scopolamine (1 mg/kg; s.c.)
F
IP Level (% control Vehicle)
LiCl (100 mg/kg; s.c.)
Pilocarpine (mg/kg; s.c.)
SKF 35393 (30 mg/kg; s.c.)